Nat. Hazards Earth Syst. Sci. Discuss., https://doi.org/10.5194/nhess-2017-172
Manuscript under review for journal Nat. Hazards Earth Syst. Sci.
Discussion started: 20 June 2017

Natural Hazards and Earth System Sciences
Open Access
Discussions

1997 Kronotsky earthquake and tsunami and their predecessors, Kamchatka, Russia

Joanne Bourgeois[1], Tatiana K. Pinegina[2]

[1]Department of Earth and Space Sciences, University of Washington, Seattle, WA 98195-1310, USA
[2]Institute of Volcanology and Seismology, FEB RAS, 9 Piip Boulevard, Petropavlovsk-Kamchatsky, 683006, Russia

Correspondence to: Joanne Bourgeois (jbourgeo@uw.edu)

Abstract. The northern segment of the Kamchatka subduction zone (KSZ) experienced three tsunamigenic earthquakes in the 20th century (Feb 1923, April 1923, Dec 1997), events that help us better understand the behavior of this segment. Characterizing these historical earthquakes and tsunamis in turn contributes to interpreting the prehistoric record, which is necessary to evaluate recurrence intervals for such events. A particular focus of this study is the nature and location of the 5 December 1997 Kronotsky rupture as elucidated by tsunami runup in southern Kamchatsky Bay. Some studies have characterized the subduction zone off Kronotsky Peninsula as less seismogenic, as indicated by gravity-anomaly analyses, and have placed the 1997 rupture south of the promontory. However, tsunami runup north of the peninsula, as evidenced by our mapping of tsunami deposits, requires the rupture to extend farther north. Previously reported runup (1997 tsunami) on Kronotsky Peninsula was no more than 2-3 m, but our studies indicate tsunami heights for at least 50 km north of the peninsula, ranging from 3.4 to 9.5 m (average 6.1 m), exceeding beach ridge heights of 5.3 to 8.3 m (average 7.1 m). For the two 1923 tsunamis, we cannot distinguish their deposits in southern Kamchatsky Bay, but they are in sum more extensive than the 1997 deposit. A reevaluation of the April 1923 earthquake (and its tsunami) suggests that its moment magnitude should be revised upward to Mw ~8. This revision makes the two 1923 events more like a pair, with the 1997 earthquake filling a gap between them. Deeper in time, the 1700-year prehistoric record of tsunamis in southern Kamchatsky Bay indicates that during this interval, there were no local events significantly larger than the 20th century earthquakes. Together, the historic and prehistoric record suggests a more northerly location of the 1997 rupture, a revision of the size of the April 1923 earthquake, and agreement with previous work suggesting the northern KSZ ruptures in smaller sections than the southern KSZ. The latter conclusion requires caution, however, as we continue to learn that our historic and even pre-historic records of earthquakes and tsunamis is limited, in particular as applied to hazard analysis. This study is a contribution to our continued efforts to understand tectonic behavior around the northern Pacific and in subduction zones, in general.

Key words: Kamchatka, subduction zone, 1997 Kronotsky earthquake, 1997 Kronotsky tsunami, Kamchatsky Bay, paleotsunami, paleoseismology

Nat. Hazards Earth Syst. Sci. Discuss., https://doi.org/10.5194/nhess-2017-172
Manuscript under review for journal Nat. Hazards Earth Syst. Sci.
Discussion started: 20 June 2017

Natural Hazards and Earth System Sciences
Discussions

1 Introduction

References to the modest or small tsunami of 15 December 2006 central Kurils (Ammon et al., 2008; Liu, 2009), when in fact this tsunami generated an average of 9.6 m runup over an along-rupture length of 390 km (MacInnes et al., 2009), remind us that without post-tsunami or tsunami-deposit surveys, remote spots in the world may experience large events without a written record. The case of the 5 December 1997 tsunami following the Mw 7.7-7.9 Kronotsky earthquake (Fig. 1, Fig. 2), however, is even more complex historically, because there *was* a post-tsunami survey quickly following (Zayakin and Pinegina, 1998), though of limited extent. The local tide-gage record for this 1997 tsunami is also incomplete, and deep-water pressure recorders deployed at the time were not positioned to get distinctive recordings from a tsunami originating near Kronotsky Cape (Bourgeois and Titov, 2001). The earthquake and tsunami occurred in the dark of a December night in an area with no permanent settlements.

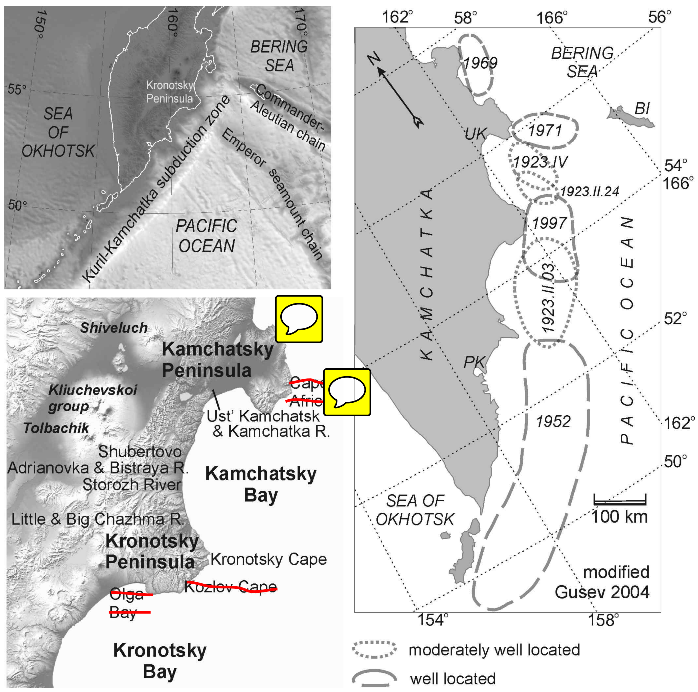

Figure 1. General tectonic setting and locations. **Upper left**: Major topography of and bathymetric features around Kamchatka. **Lower left**: locations of sites mentioned in text and tables. **Right**: Interpreted rupture locations of 20th century tsunamigenic (except *1923.II.24*) earthquakes along the Kamchatka portion of the Kuril-Kamchatka subduction zone (modified from Gusev , 2004, Fig. S1; Martin et al., 2008). ~~The rupture area of the 1997 earthquake varies in different analyses, one of the subjects of this (our) paper; also discussed are the 1923 earthquakes.~~ PK = Petropavlovsk-Kamchatsky; UK = Ust-Kamchatsk; BI = Bering Island.

In the summer of 2000, we conducted a field survey for historical and paleo- tsunami deposits in south Kamchatsky Bay (Fig. 1), north of Kronotsky Peninsula. We expected to find evidence of historical Kamchatka tsunamis such as 1923 (Table 1; Table S1), but not for 1997 Kronotsky because on the southern Kronotsky Peninsula, the post-tsunami survey found evidence of quite limited runup. Thus we were surprised to find a sand layer just at the surface, covered only by plant debris such as grass and leaves, distributed much as we have come to expect of tsunami deposits, and at elevations of 5 m or more above sea level. No alternative other than a tsunami from the 1997 earthquake and its aftermath could explain the layer and its distribution.

Nat. Hazards Earth Syst. Sci. Discuss., https://doi.org/10.5194/nhess-2017-172
Manuscript under review for journal Nat. Hazards Earth Syst. Sci.
Discussion started: 20 June 2017

Natural Hazards and Earth System Sciences
Open Access
Discussions

The implications of this case, where an earthquake was analyzed without full knowledge its tsunami, are several. First, the fact that there was runup greater than that reported by a post-tsunami survey changes our view of the tsunami as well as of the earthquake. Further, the size of the tsunami, based on its deposits and a corroborating eyewitness account (acquired in 2001), constrains the rupture characteristics of this earthquake. The tsunamigenic portion of this earthquake was in a "gap" between two 1923 tsunamigenic earthquakes, at least one of which was locally larger than 1997.

This recent historical tsunami also helps us interpret earlier historical ~~and~~ well as prehistoric earthquakes and tsunamis along the northernmost part of the Kuril-Kamchatka subduction zone. Tsunamis originating from this region commonly have an impact not only locally but also on Hawaii, as did the February 1923 tsunami, and in some cases even on the western coast of the Americas, as did the 2006 central Kurils tsunami.

2 Background

2.1 The 1997 Kronotsky earthquake

On 5 December 1997 at 23:26:51 local time (11:26:51 UTC), a large earthquake (Mw 7.7-7.9; we use 7.8) shook the region of the Kronotsky Peninsula, Kamchatka, Russia (Fig. 1, Fig. 2; Gordeev et al., 1998). The earthquake was characterized by a typical foreshock-mainshock-aftershock sequence (Gusev et al., 1998; Fedotov et al., 1998; Balakina, 2000; Zobin and Levina, 2001; Kuzin et al. 2007; Slavina et al., 2007). Most studies of the earthquake calculate a moment magnitude of 7.8 for the energy released in the first 60-80 seconds of the main rupture (e.g., Zobin and Levina, 2001). Gusev and Shumilina (2004), in reassessing many Kamchatka earthquakes, assign Mw 7.9 to Kronotsky 1997. In addition to the mainshock, and using GPS measurements, Gordeev et al. (2001) calculate Mw 7.7 for deformation in the *pre-seismic* half month, and approximately Mw 7.9 for *post-seismic* deformation; Bürgmann et al. (2001) calculate Mw 7.7 of (*post-seismic*) aseismic energy release in the 2 months following the mainshock, also based on GPS data.

The locations of the mainshock and of any slip concentration for this earthquake have not been well resolved, and with one early exception (Sohn, 1998), locators have not used tsunami data. Based on seismic data, the locations of foreshocks and the mainshock/epicenter (Fig. 2) are in the northern part of the interpreted rupture area. A number of analytical locations of the mainshock lie under the NE Kronotsky Peninsula (Fig. 2; Table S2). Some analyses interpret the rupture to have propagated NE to SW (Petukhin et al., 1998), deepening toward the SW. Gusev (2004) maps the entire aftershock zone as part of the 1997 event (Fig. 1). On the other hand, the linear zone of aftershocks in the SW (Fig. 2) has been interpreted to be a separate stress zone (Kuzin et al., 2007) potentially along a separate transverse fault (Slavina et al., 2007). In an analysis focused on GPS data, Bürgmann et al. (2001) place the majority of the primary rupture energy in the southern half of the aftershock zone.

Nat. Hazards Earth Syst. Sci. Discuss., https://doi.org/10.5194/nhess-2017-172
Manuscript under review for journal Nat. Hazards Earth Syst. Sci.
Discussion started: 20 June 2017

Natural Hazards and Earth System Sciences
Discussions

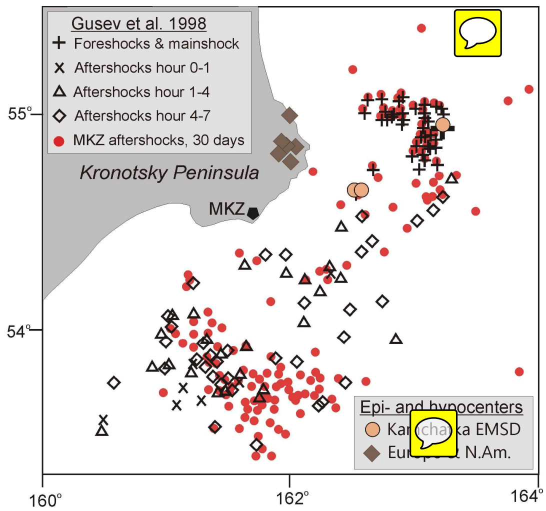

Figure 2. Foreshocks (3-5 Dec 1997), mainshock and aftershocks of the 5 December 1997 Kronotsky earthquake (Gusev et al., 1998). Plotted foreshocks and MKZ aftershocks include only cases where P and S arrivals could be read from records of the nearest station, MKZ. Locations of epicenters and hypocenters are from various analyses, both local and farfield as reported from the International Seismological Center (Table S2). Slavina et al. (2007) interpret the southwestern aftershock activity to be on a separate, transverse fault; Kuzin et al. (2007) also interpret the SW portion of the (extended) aftershock region to be a separate stress zone

2.2 The recorded 1997 Kronotsky tsunami

The most complete contemporary record of the 1997 Kronotsky tsunami is from far-field tide gages. Both proximal tide gages, in Ust' Kamchatsk and in Nikolskoe (Bering Island) (Fig. 1), were not functioning when the tsunami arrived. The Petropavlovsk-Kamchatsky gage is very protected and shows a wave train with an amplitude of about 0.01 m (Zayakin and Pinegina, 1998). The tide gage at Nikolskoye resumed recording after the first 10 hours of the tsunami, with a few cm of amplitude remaining (Zayakin and Pinegina, 1998). The far-field tsunami had tide-gage amplitudes in Alaska/Aleutians and Hawaii in line with other tsunamis traveling to Hawaii from the Russian Far East (Table S3; Fig. S4). The tsunami was recorded on at least 12 tide gages (Table S3), with the highest amplitude (half of wave height) of 0.3 m at Kahului, Maui, Hawaii. Deep-water pressure sensors deployed at that time in the north Pacific were all in tsunami shadows for this tsunami source, and in all cases, the modeled and measured tsunami was within the noise level of the buoys (Bourgeois and Titov, 2001; no event page at http://nctr.pmel.noaa.gov/database_devel.html).

A truncated post-earthquake and tsunami survey by helicopter took place on 9 December 1997 (Leonov, 1998; Zayakin and Pinegina, 1998). The survey reached as far north as Kronotsky Cape on the Kronotsky Peninsula (Fig. 1) and found that the tsunami had not exceeded the unvegetated beach. At this time, the beach was covered with a thin layer of ice and snow, which in places had been coated by the tsunami with a thin sand layer and elsewhere had been broken up by the tsunami (Fig. 3). The team did not have surveying equipment and estimated runup to be no more than 3 m (T. Pinegina notes), and the published report gave a maximum of 1-1.5 m. The turnaround point in the survey was dictated by fuel and available daylight.

On 5 December 1997, two rangers were in a cabin near Big Chazhma River; one of them was interviewed (in Petropavlovsk-Kamchatsky) by T. Pinegina 19 April 2001. They felt the earthquake that night, and the next day, as was their custom, they went via snowmobile to survey the northern coastal part of Kronotsky reserve, to the Little Chazhma River area. At the mouth of the Big Chazhma, they saw jumbled ice and seaweed on the snow; a cabin on

Nat. Hazards Earth Syst. Sci. Discuss., https://doi.org/10.5194/nhess-2017-172
Manuscript under review for journal Nat. Hazards Earth Syst. Sci.
Discussion started: 20 June 2017

Natural Hazards and Earth System Sciences
Open Access
Discussions

the south bank of the Little Chazhma River was partly wetted, and there was seaweed on the snow. Normally the rangers crossed the river near this cabin, but the river was a jumble of ice and they had to go some distance upstream in order to cross (on ice). On the other side, they could not continue north because there was water in the low spot between beach and hill (see Fig. 4, our profile 100).

Based on results of the post-tsunami survey (reported to Sohn by V. Gusiakov), Sohn (1998) analyzed the tsunami with regard to its earthquake source and concluded that the main rupture must have lain largely under land, in order to explain the low runup accompanying a moment magnitude she calculated as Mw 7.7. However, the tsunami amplitudes on tide gages in Hawaii indicate that there was substantial subsea deformation.

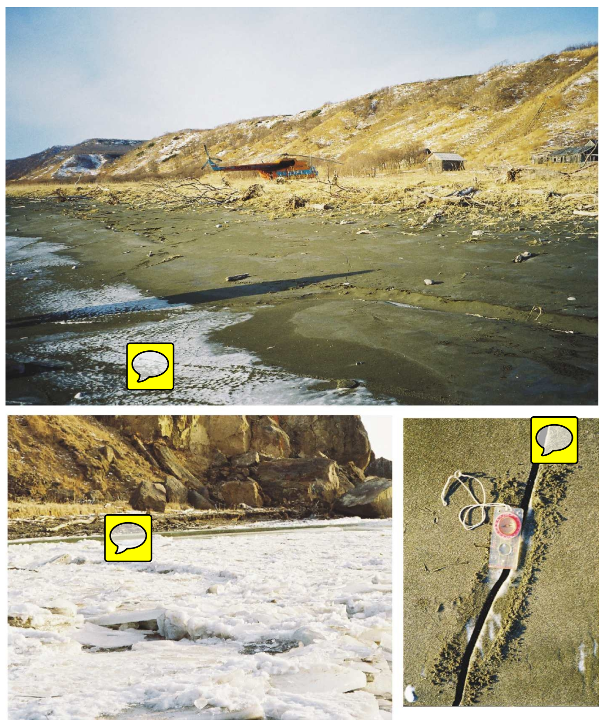

Figure 3. Photos taken by T. Pinegina on 9 Dec 1997 near Kronotsky Cape (location on Fig. 1). For additional photo and sketch for context, see Fig. S3. **Above**: the tsunami deposited sand ~~on~~ above the snow up to about the line of grassy vegetation at the back of the beach (helicopter for scale). **Lower left**: Ice and snow broken up by the tsunami (excerpted from photo in Fig. S3). **Lower right**: detail of tsunami-deposited sand above snow that covered the beach. Compass for scale.

2.3 Historical record of earthquakes and tsunamis affecting the field area

The Kamchatka Peninsula has a short but rich historic record of large earthquakes and attendant tsunamis, of which we discuss herein only 20th century tsunamis originating in or having been recorded in the field region of southern Kamchatsky Bay (Table 1). In addition to locally originating tsunamis, Kamchatka is vulnerable to tsunamis originating from Chile, less so from Peru, and not so much from Japan, Alaska, Aleutians and Central America, due to directivity (e.g., see Table S1). ~~Based on existing scant records in the vicinity of the field area (Table 1), we can expect the 1960 Chile tsunami to have reached elevations of 3-5 m above sea level in the field area,~~ on the order of twice as high as the 1952 southern Kamchatka tsunami *at these same localities*.

Nat. Hazards Earth Syst. Sci. Discuss., https://doi.org/10.5194/nhess-2017-172
Manuscript under review for journal Nat. Hazards Earth Syst. Sci.
Discussion started: 20 June 2017

Natural Hazards and Earth System Sciences
Open Access
Discussions

Table 1. 20th CENTURY TSUNAMIS AFFECTING THE KAMCHATSKIY BAY COAST OF KAMCHATKA*

EARTHQUAKE PARAMETERS			RECORDS OF TSUNAMI RUNUP (*tide gage records in italics*) in meters										
			Locations South to North (see Figure 1)										
Date (local)	Source region	Mw	Kron Bay	Kron. Cape	**Chazhma - Adr-Bistr R.**	Shuber-tovo	1st River s. of U-K	Tsutsumi s. of U-K	*U-K tide gage*	Dembi Spit, U-K	Bering I. (south)	MAX KAM	Hilo, HI
5-Dec-97	**Kronotsky Peninsula**	**7.8/7.9^**	**0.5-1**	**1.5**	**this paper**				***gage broken***		***incompl record***	**this paper**	***0.24***
15-Dec-71	Commander Is.	7.8^							*0.47*				*0.10*
23-Nov-69	Bering Sea	7.7							*0.2*			10-15	*0.10*
24-May-60	**Chile**	**9.5**	**4**				**3**		***0.8***	**3-4**	**3-3.5**	**7**	**~10**
05-Nov-52	**s. Kamchatka**	**9**	**10-13**			**0.5-1**			***0.1***		**2**	**10-15**	***1.1***
14-Apr-23	**Kamchatskiy Bay**	**7.3/8.2^**					**20**	**>5**		**11#**	**4**	**20**	***0.30***
04-Feb-23	**Kronotskiy Bay**	**8.5^**	**6-8**		**4-5 km up Chazhma**			**~4**				**6-8**	**6.10**

*Bold: **tsunamis most likely to leave a sedimentary record in south Kamchatsky Bay**; see Supplemental Table 1 for a more complete list of tsunamis and Supplemental Table 4 for specifics in 1923 cases. Primary sources: Zayakin and Luchinina, 1987; NCEI (formerly NGDC) Natural Hazards Data, online (see references)

^Kamchatka Mw's from Gusev and Shumilina, 2004; G&S 8.2 for 14Apr23 is based on tsunami; see text discussion
#The 20-m and 11-m numbers are from higher-relief shorelines than the other measurements

The largest documented local tsunamis from earthquakes near Kronotsky Peninsula (Fig. 1; Table 1) are two from 1923, both having local as well as farfield records (Table S4); both may have been large in south Kamchatsky Bay. There was also a 24 Feb 1923 Mw 7.6 earthquake in this area (Fig. 1; Gusev, 2004); however, it has no historical tsunami record in the near or far field. [The Mw 8.0 1917 earthquake along the Bering fracture zone (Fig. S1) also did not produce an observed tsunami.] The 3 Feb 1923 Kronotsky Bay earthquake (Mw 8.5) was located south of Kronotsky Cape (Fig. 1). The 14 April 1923 north Kamchatsky Bay earthquake (Mw 7.3 in NCEI catalogue) generated a high tsunami near Ust-Kamchatsk (Table 1; Table S1). Based on tsunami amplitudes, Gusev and Shumilina (2004) suggested this April 1923 earthquake had a moment magnitude of 8.2 (Table S1, Fig. S2). Based on the estimated locations of the February and April sources (Fig. 1) and the recorded tsunami runup in Ust-Kamchatsk (Table 1), we might reason that in south Kamchatsky Bay the April 1923 tsunami may have been larger. However, Zayakin and Luchinina's catalogue records that the February 1923 tsunami went 4-5 km up the Chazhma River (Table 1).

The record of earthquakes and tsunamis on Kamchatka prior to the 20th century is spotty but improving (Zayakin and Luchinina, 1987; Godzikovskaya, 2010); ~~the earthquake catalogue from the second half of the 19th century is not as complete as from before or after~~ (Gusev and Shumlina, 2004). Earthquakes on 17 May 1841 and 17 October 1737 originated in the region of the 1952 south Kamchatka great earthquake, so likely did not have significant effect in southern Kamchatsky Bay (see Table 1, 1952 runup). Other tsunamis that may have affected south Kamchatsky Bay are an autumn 1849 tsunamigenic earthquake in the vicinity of the Komandorsky Islands (Godzikovskaya, 2010) and a 1791 event which has an intriguing account of having affected the mouth of the Kamchatka River (Ust-Kamchatsk), reaching 7 km upstream (Zayakina and Luchinina, 1987).

Nat. Hazards Earth Syst. Sci. Discuss., https://doi.org/10.5194/nhess-2017-172
Manuscript under review for journal Nat. Hazards Earth Syst. Sci.
Discussion started: 20 June 2017

3 Methods

We measured 15 topographic profiles (Fig. 4) perpendicular to the shoreline along the coast of southern Kamchatsky Bay (Fig. 1), and made 117 excavations along these profiles in order to document historical and paleotsunami deposits. We used a surveying rod with a transit level (hand level and tape for profile 001 and upper part of profile 120) (methods as in Bourgeois et al., 2006).

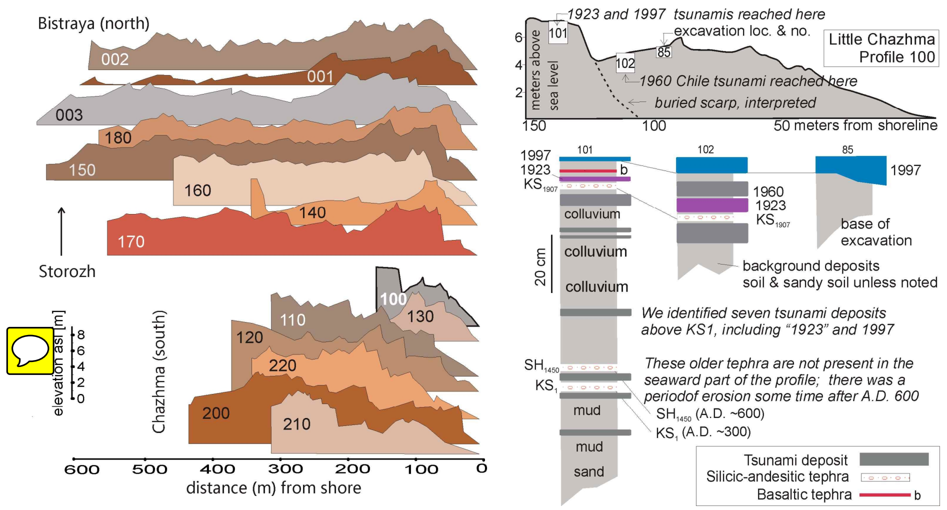

Figure 4. Left. Topographic profiles measured in southern Kamchatskiy Bay (locations on Fig. 1, arranged from south (bottom) to north (top), except 001 and 002 reversed to reveal topography. Distances and elevations are measured from 0 at the water line, corrected to low tide. **Right**: Chazhma Profile 100 used as a key to collected profile data and interpretations *(interpretation in italics)*; background deposits are soil or sandy soil, unless noted.

Tsunamis create sedimentary deposits as they flood the coast with turbulent, turbid water. The general characterization of a tsunami deposit in sandy coastal systems is a sand sheet that typically thins and fines landward, following topography (Bourgeois, 2009). Many factors, from sediment availability to coastal topography and roughness to the velocity profile of incoming and outgoing waves, play a role in sedimentation. Kamchatka field sites are primarily sandy, vegetated coastal plains and associated peat marshes, where availability of sand and the vegetative cover maximize the likelihood of generating and preserving tsunami deposits. (Many historical Kamchatka tsunamis have occurred during winter snow cover; deposits would have been "let down" onto a vegetative mat as the snow melted.) The maximum distance inland of a tsunami deposit (*sediment inundation*, Fig. 5) and the deposit's elevation at sediment inundation (*sediment runup*, Fig. 5) represent minimum estimates of tsunami extent for several reasons. Tsunami deposits can only be more limited (not more extensive) than water runup and inundation, the final limit of a deposit is not always located in the field, and thin deposits may not be identified or preserved.

Nat. Hazards Earth Syst. Sci. Discuss., https://doi.org/10.5194/nhess-2017-172
Manuscript under review for journal Nat. Hazards Earth Syst. Sci.
Discussion started: 20 June 2017

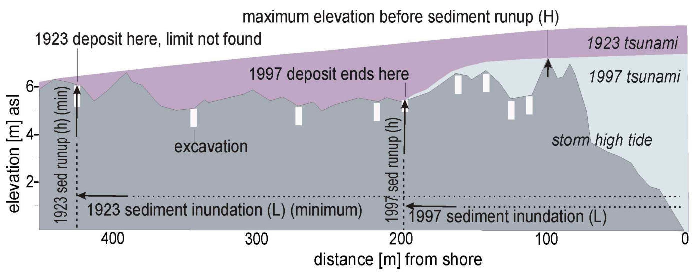

Figure 5. Terminology for sediment runup and sediment inundation, and interpretation of deposits from 1997 and 1923, using example of an actual profile (Storozh 160; vertical exaggeration ~10). Note that near the shoreline, both tsunamis had to exceed a point (H) higher than "sediment runup" (h) and that, although the minimum sediment runup for 1923 is not much greater than for 1997, 1923 had to have been higher to generate greater inundation. Distances and elevations are from surveying.

Primary age control in excavations is provided by dated regional and local marker tephra layers (Table 2), which in general have been well studied on Kamchatka (e.g., Braitseva et al., 1997), although tephra in the south Kamchatsky Bay area had not previously been examined. Based on our own and previous work, as well as on more recently published isopach maps (Kyle et al., 2011; Ponomareva et al., 2017), the three most consistently present layers in the sections are $KSht_3$ (A.D. 1907 — we label KS_{1907} on diagrams)—most useful for studying the historical record, SH_{1450} (A.D. ~600) and KS_1 (A.D. ~300), the latter used as the lower boundary for our tsunami statistics. In more northern profiles, SH_2 (A.D. ~1130) is commonly present. Recent work around Shiveluch volcano and Kamchatsky Peninsula (Fig. 1) has led to redesignation of Shiveluch tephras and to more definitive model ages of these tephra (Ponomareva et al., 2017). In addition to the silicic marker tephra (Table 2), there are local basaltic-andesitic tephra layers, which can be from Kliuchevskoi, Bezymianny, Tolbachik or Gamchen volcanoes; we used these tephra only as local field guides. In the northernmost of our profiles, a historic ash from Bezymianniy 1955 (year before the 1956 paroxysmal eruption) is locally present and a factor in distinguishing the Kamchatka 1952 from the Chile 1960 tsunami deposits.

Table 2. Marker tephra layers younger than 2000 years old in shoreline profile sections, southern Kamchatsky Bay*

Code Field/Classic^	Code New*	Source volcano	Modeled age* (years B.P.)	Assigned age* (calendar years)	Field description	Field thickness
$KSht_3$	$KSht_3$	Ksudach	Historical	A.D. 1907	Light to medium gray, fine to very fine sand	0.5-2 cm
SH_2	SH#6	Shiveluch	817 +59/-57	A.D. 1134	White (faint gray, yellow white), fs-vfs, has pumice	0.5-1 cm; distinct toward north
SH_{1450}	SH#12	Shiveluch	1356 +52/-45	A.D. 596	Pale yellow, yellow gray, lt gray, vfs-ms, salt & pepper —grainy	1-2.5 cm; typically 1-2 cm
KS_1	KS_1	Ksudach	1651 +54/-61	A.D. 298	Lt brown, beige, "coffee cream"; thin gray cap; si-vfs	1-3 cm; usually not >2 cm

*Ponomareva et al., 2017
^Braitseva et al., 1997

Nat. Hazards Earth Syst. Sci. Discuss., https://doi.org/10.5194/nhess-2017-172
Manuscript under review for journal Nat. Hazards Earth Syst. Sci.
Discussion started: 20 June 2017

Natural Hazards and Earth System Sciences
Discussions

For the prehistoric record of tsunami runup and inundation, topographic profiles would not necessarily be the same as in the recent past must be reconstructed to account for succeeding topographic changes in elevation and distance along the profile. While we cannot typically reconstruct profiles that have been changed by erosion, we can reconstruct profile progradation (building seaward), which affects profile width. Our method uses preserved tephra as discussed, e.g., in Pinegina et al. (2013) and MacInnes et al. (2016). Changes in elevation are quantified by determining the age and elevation of the lowest former soil horizon above marine sand in any excavation (as in Pinegina et al., 2013).

3.1 Field localities

The southern field site (Fig. 1), which we call "Chazhma," is a narrow strip (~400 m wide or less) of Holocene accumulative coastline along a rugged coast just north of the Kronotsky Peninsula. The two profiles near river mouths (Chazhma 210 and Chazhma 130; Fig. 4) maintain lower elevations (< 4 m) over much of their distance, though both reach elevations of more than 6 m above sea level. The other five profiles rise, typically in sharp steps indicative of Holocene uplift events (e.g., Pinegina et al., 2013), reaching typical maximum levels of 8-10 m (Fig. 4). Net uplift on these profiles is consistent with longer-term uplift of Pleistocene terraces on the Kronotsky Peninsula (Melekestsev et al., 1974).

The northern field site, which we call "Storozh," extending north to the Bistraya River (Fig. 1), is a broader strip (typically 600 m wide) of Holocene accumulative coastal plain associated with active and drowned river mouths. Two of these profiles (140, 001) drop in elevation behind one or more beach ridges (Fig. 4). The other seven profiles are typified by a series of beach ridges, of which the seaward ridges are higher, reaching typically 6-7 m, with an average elevation of the profile in the range of 4-6 m (Fig. 4). Such profiles indicate ~~mild subsidence~~ or no vertical change in the late Holocene.

4 Results -- 20th century tsunami deposits

In field season A.D. 2000, the sand we interpret to have been deposited by the 1997 Kronotsky tsunami formed a sheet-like layer at the surface, buried only by grass, leaves and other dead vegetation. The deposit we interpret to be "1923" (from one or both of two tsunamis in 1923) lies above the marker tephra KS_{1907} with less soil thickness between KS_{1907} and "1923" than between the top of "1923" and the base of the modern turf. Our interpretation of "1923" as well as a rare sand layer between "1923" and 1997, which we assign to the 1960 Chile tsunami, is discussed below.

Using identified and mapped tsunami deposits, we calculate minimum sediment runup and inundation on each of the 15 profiles (Table 3, Figure 6), correcting for tide at the time of survey. We determine minimum sediment runup (h) by the presence or absence of distinct 1997 and "1923" deposits on each profile. We distinguish between profiles where the farthest landward excavation still contains the 1997 or "1923" deposit and ones that do not. If no deposit is present in one or more excavations landward of ones with a deposit, the limit of sediment inundation (L) occurs within the measured profile (Fig. 5, example of 1997) and actual tsunami runup is estimated from sediment runup. For profiles where a particular tsunami deposit extends beyond all excavations (Fig. 5,

Nat. Hazards Earth Syst. Sci. Discuss., https://doi.org/10.5194/nhess-2017-172
Manuscript under review for journal Nat. Hazards Earth Syst. Sci.
Discussion started: 20 June 2017

Natural Hazards and Earth System Sciences
Open Access
Discussions

example of 1923), the actual size of the tsunami could be, in some cases, significantly greater than our sediment-runup and inundation minima. We also report the maximum height the tsunami had to exceed (H) as it traveled along (across) a profile. Note that maximum elevations and inundation distances are affected by elevations and distances along actual profiles (Fig. 4). In a few cases, the farthest inland excavation was at a low elevation that could have been reached via the river rather than over the profile (Table 3, Fig. 6).

4.1 1997 tsunami

Sediment runup data (Table 3, Fig. 6) indicate that north of the Kronotsky Peninsula the 1997 Kronotsky tsunami ran up to as much as 9.5 m, averaging 6.1 m, with moderate inundation distances of 100-300 m. The general pattern over about 100 km of coastline, including post-tsunami survey observations on Kronotsky Peninsula itself, is relatively smooth. The maximum elevation reached by the tsunami deposit is higher on southern (Chazhma) profiles. However, lower runup numbers on northern profiles may be an artifact of their lower elevations (Figure 4); inundation distances are greater on these profiles (Table 3). On some profiles the 1997 deposit is absent.

4.2 1923 tsunamis

Sediment runup and inundation data for “1923” indicate that this tsunami was larger than 1997. The deposit we interpret as from 1923 is usually thicker and more extensive, and never less extensive, than the deposit from 1997. The “1923” deposit is present on all measured profiles whereas the 1997 deposit is missing on six (Table 3, Fig. 6). Only on profiles where the sediment limit was not found (e.g. 100), or where profiles dropped to low elevations at their landward extent (001, 180, 160, 140, 100, 130, 210) were “1923” deposits at similar or lower elevations than 1997, and in many of these cases (001, 180, 160, 130), inundation distances for “1923” were longer. Even in the few cases where our field observations did not distinguish the two by sediment runup or inundation, the “1923” deposit was coarser and/or thicker than 1997.

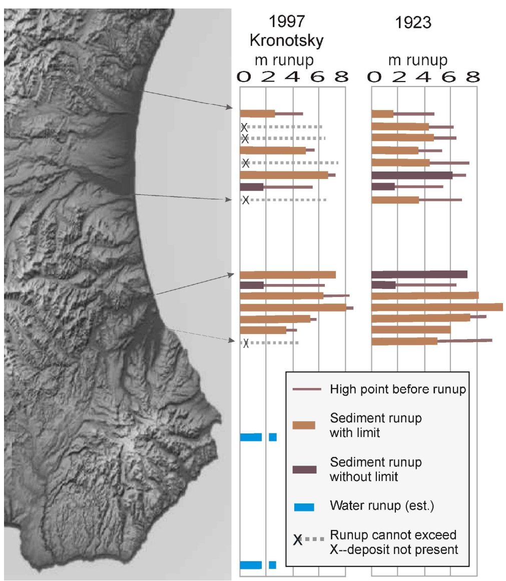

Figure 6. Water (Zayakin and Pinegina, 1998) and sediment runup (this paper, Table 3) for the 1997 Kronotsky tsunami on and north of the Kronotsky Peninsula, southern Kamchatsky Bay (locations on Figure 1). Water runup was not measured with instruments but estimated; tsunami did not exceed the unvegetated beach (e.g., Fig. 3); it could have been somewhat higher than reported, shown by dashed blue line. Sediment runup is also illustrated for the tsunami deposit closely above KS_{1907}, which we interpret as from 1923 February or April (see text discussion). Sediment inundation is given in Table 3, as well as latitudes and longitudes for the 15 profiles. Figures 4 and 5 illustrate methods and terminology.

Nat. Hazards Earth Syst. Sci. Discuss., https://doi.org/10.5194/nhess-2017-172
Manuscript under review for journal Nat. Hazards Earth Syst. Sci.
Discussion started: 20 June 2017

Natural Hazards and Earth System Sciences
Open Access
Discussions

Table 3. Sediment runup and inundation for historical tsunamis above KS_{1907}, southern Kamchatsky Bay

				1997			1960			1923		
Region	Profile #	Latitude	Longitude	h	L	H	h	L	H	h	L	H
Bistraya River	001	55.6226	161.7799	3.4	200	5.3	3.3	**126**	5.3	2.0	250	5.3
	001 via river									0	**650**	*
Bistraya River	002	55.59735	161.76802							4.4	205	6.2
	002 via river									2.2	560	*
Bistraya River	003	55.57814	161.76001							4.8	211	6.5
Adrianovka R.	180	55.52745	161.74836	4.8	118	5.6				3.5	367	5.6
Storozh River	150	55.48508	161.74135							2	645	7.7
Storozh River	160	55.45819	161.73936	6.6	159	7.5	**6.2**	107	7.5	6.1	419	7.5
Storozh River	140	55.4387	161.7393	5.8	**330**	5.8				5.8	330	5.8
Storozh River	170	55.38604	161.73401							3.6	267	6.7
Little Chazhma R.	100	55.1407	161.8281	7.4	125	7.4	4.5	107	6.2	7.4	125	7.4
Little Chazhma R.	130	55.1235	161.8379	4.4	109	6.3	4.4	78	5.1	1.8	158	6.3
Chazhma	110	55.1181	161.8408	6.6	200	8.3				8.1	315	8.3
Chazhma	120	55.1019	161.8514	**9.5**	200	9.5				**12**	380	9.5
Big Chazhma R.	220	55.0794	161.8679							7.7	335	9.8
Big Chazhma R.	210	55.071	161.876	6.0	305	8.0				6	305	8
Big Chazhma R.	200	55.0629	161.8879							6.6	361	9.1
	200 via river									5	428	*
			AVERAGES	*6.1*	*194*	*7.1*	*4.6*	*105*	*6.0*	*4.9*	*346*	*7.3*

h - elevation of excavation m a.s.l.; equals "sediment runup" (maxima in bold)

L - distance from the shoreline, m; equals "sediment inundation" (maxima in bold)

H - highest elevation, m a.s.l., between shoreline and excavation; must be exceeded where there is a deposit (max. in bold)

**If* the tsunami reached a low inland point via the river (indeterminate), H from the profile is not relevant.

4.3 Chile1960 deposit

Between "1923" and 1997 deposits on a few profiles (Table 3), there is a thin, patchy and less extensive deposit which we attribute to the 1960 Chile tsunami (e.g., Fig. 4, right). We favor 1960 over 1952 Kamchatka because the 1960 tsunami was larger than 1952 in the Kamchatsky Bay region (Table 1). Also, The more locally generated 1952 tsunami dies off in amplitude along strike of the rupture (MacInnes et al., 2010), whereas the Chilean tsunami on Kamchatka is little affected by latitude (Zayakin and Luchinina, 1987). Supporting the 1960 interpretation, in one excavation on profile 001, this intermediate tsunami deposit lies above the Bezymianny 1955 tephra layer.

4.4 Historical tsunami deposit close below KS_{1907}

In many excavations (e.g., Fig. 7), there is a tsunami deposit within a few cm of the base of $KSht_3$ and which is comparable to 1997 and 1923 in thickness and extent. Although pre-1907 sedimentation rates are difficult to determine this tsunami deposit must fall within the historical period, which extends back to 1737. However, the more complete historical records are from southern Kamchatka, and the second half of the 19th century record is particularly spotty (Gusev and Shumulina, 2004). Thus we cannot assign a specific event to this deposit.

Nat. Hazards Earth Syst. Sci. Discuss., https://doi.org/10.5194/nhess-2017-172
Manuscript under review for journal Nat. Hazards Earth Syst. Sci.
Discussion started: 20 June 2017

Natural Hazards and Earth System Sciences Open Access Discussions

5 Discussion – 1997 and "1923" Deposits

5.1 1997 tsunami

Our observations are consistent with 1997 being a seismogenic tsunami source with significant rupture energy expended in the northern portion of the zone of aftershocks. The extensive and relatively smooth distribution of runup (Table 3; Fig. 6) and the ratio of maximum runup to distance over which the tsunami had significant runup (on the order of 10^{-5}) indicate that this tsunami was typical of a seismogenic source rather than a landslide source (cf. Okal and Synolakis, 2004). The far-field tide-gage records (e.g., Hilo, Table 1) are also indicative of a broad rather than a point source. Given that the post-tsunami survey reported runup that did not exceed the beach on the Kronotsky Peninsula and that the deposits we mapped north of the peninsula are from the 1997 tsunami, *any source model must explain low runup on the peninsula and relatively high runup north of the peninsula*. Source region models by Bürgmann et al. (2001) and Llenos and McGuire (2007), e.g., do not include the northern aftershock area, and such models have been used to interpret Kamchatka subduction-zone behavior (e.g., Song and Simons, 2003; Bürgmann et al., 2005; Llenos and McGuire, 2007; Bassett and Watts, 2015). On the other hand, source regions by Gusev et al. (1998; also Gusev, 2004) and Levina et al. (2013) tend to include the entire aftershock zone, overlapping Feb 1923 in the south but also filling the gap between Feb 1923 and April 1923 (Fig. S1). Zobin and Levina (2001) favor most mainshock energy being generated in the middle zone defined by fewer aftershocks (see Fig. 2); Slavina et al. (2007) interpret the southwestern aftershock activity (Fig. 2) to be on a separate, transverse fault; Kuzin et al. (2007) also interpret the SW portion of the (extended) aftershock region to be a separate stress zone. A recently published finite fault model ~~resolves to most~~ ~~deformation~~ being under the Kronotsky Peninsula, with most energy release focused in the north (Hayes, 2017; https://earthquake.usgs.gov/earthquakes/eventpage/usp0008btk#finite-fault).

5.2 1923 tsunamis

There are reasons to favor either or both the 3 February 1923 and the 13 April 1923 Kamchatka tsunamis as the generator(s) of the deposit above KS_{1907} that we identify as "1923." Given what is known, south Kamchatsky Bay is the place most likely to have *comparable* runups from each. Both tsunamis have a record in Hilo, but one is runup and the other tide-gage amplitude (Table 1). There is no case on Kamchatka of a pair of similarly measured records from the same locality with which to compare the two tsunamis, with the exception of observations that the April tsunami generated more damage at the Tsutsumi fish plant southeast of Ust-Kamchatsk (Table S4). The 3 February tsunami was larger in most catalogued locations (Table S4) but apparently smaller than April 1923 in *north* Kamchatsky Bay. The two 1923 tsunamis both occurred while the ground would have been snow covered so that following snowmelt, it would be nearly impossible to distinguish two different deposits in this case. The source regions of the two 1923 Kamchatka tsunamis have been mapped (Fig. 1) but are not easy to constrain in detail other than that the February earthquake was south of Kronotsky and the April earthquake north of it. The February earthquake has been catalogued as Mw 8.3 and the April earthquake as Mw 7.3 (Table S3), but the local and far-field tsunami runup for April 1923 suggests it was significantly larger (Gusev and Shumilina, 2004); Gusev suggests

Mw 8.2 for the April earthquake. A moment magnitude around 8 would be more consistent with its tide-gage amplitude in Hilo (Fig. S2).

5.3 Chile1960 deposit

Between "1923" and 1997 deposits ~~on a few profiles~~ (Table 3), there is a thin, patchy and less extensive deposit which we attribute to the 1960 Chile tsunami (e.g., Fig. 4, right). We favor 1960 over 1952 Kamchatka because the 1960 tsunami was larger than 1952 in the Kamchatsky Bay region (Table 1). Also, the regionally generated 1952 tsunami decreases in amplitude toward the north on Kamchatka (Zayakin and Luchinina, 1987; also see MacInnes et al., 2010), whereas the distally generated Chilean tsunami on Kamchatka is little affected by latitude. Supporting the 1960 interpretation, in one excavation on profile 001, this intermediate tsunami deposit lies above a Bezymianny 1955 tephra layer (Fig. 7).

5.4 Historical tsunami deposit close below KS_{1907}

In many excavations (e.g., profile 100 in Fig. 4, Profile 110 in Fig. 8), there is a tsunami deposit within a few cm of the base of KS_{1907} and which is comparable to 1997 and 1923 in thickness and extent. Although pre-1907 sedimentation rates are difficult to quantify this tsunami deposit must fall within the historical period, which extends back to 1737. However, we cannot assign a specific event to this deposit; the more complete historical records are from southern Kamchatka, and the second half of the 19th century record is particularly spotty (Gusev and Shumulina, 2004).

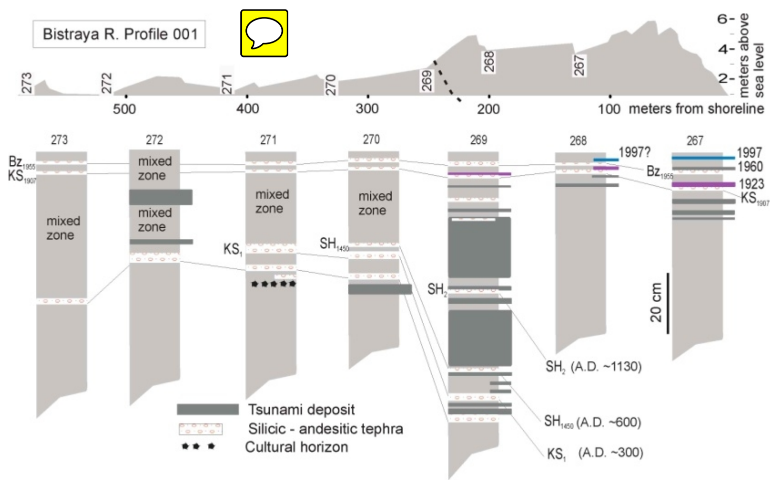

Figure 7. Northernmost profile, southern Kamchatsky Bay (Fig. 1 location; more extensive key in Fig. 4). This profile shows evidence of subsidence through time -- the landward part of the profile is lower. This lower profile has been subjected to river erosion -- the "mixed zone" is mostly fluvial sediment containing clasts of older material. Excavations having this mixed zone (273 to 270) all contain a tephra older than KS_1, indicating that older strata are preserved below the reworked material. In this profile 001, there is an ash layer from the 1955 eruption of Bezymianny, a year before its major eruption. With this tephra present, we can assign the tsunami deposit above (in excavation 267) to Chile 1960 rather than to Kamchatka 1952.

Nat. Hazards Earth Syst. Sci. Discuss., https://doi.org/10.5194/nhess-2017-172
Manuscript under review for journal Nat. Hazards Earth Syst. Sci.
Discussion started: 20 June 2017

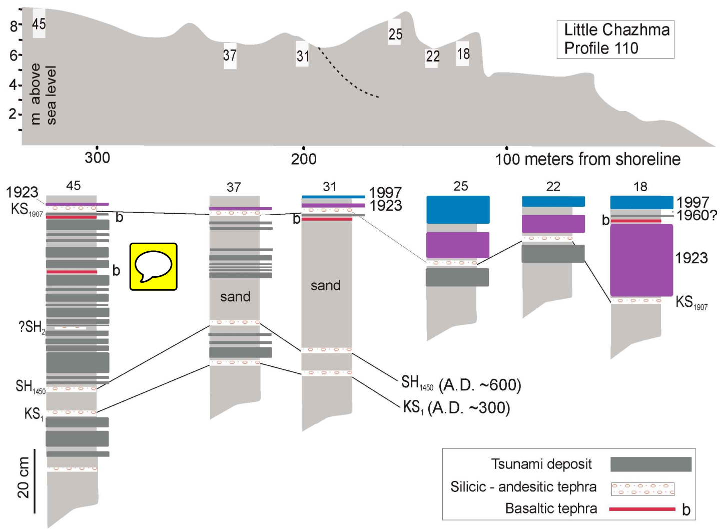

Figure 8. Profile 110, Chazhma area (Fig. 1 location; more extensive key in Fig. 4). This profile has been uplifted through time – the landward part of the profile is higher. Exc. 45 contains many tsunami sand layers currently at high elevation, which when reconstructed were lower (Fig. S5).The profile shows the distribution of 20th century deposits, as well as a tsunami deposit very close below KS_{1907}. The 1923 tsunami(s) reached the highest point shown on this profile, whereas 1997 and "below KS_{1907}" were smaller. The deposit we tentatively assigned to Chile 1960 on this profile is not included in Table 3 because the deposit was not well preserved; it is higher than any other excavation containing a deposit we attribute to Chile 1960.

6 Tsunami deposits pre-20th century back to KS_1 (~A.D. 300)

Goals in reconstructing paleotsunami history include both scientific and practical objectives. Scientifically, southern Kamchatsky Bay paleotsunamis can help us see patterns of subduction zone behavior. Are the historical tsunamis (and their generating earthquakes) comparable to events in the past? What is the "typical" event and what are the rupture patterns of the northern Kamchatka subduction zone? Practically, these questions apply also to probabilistic hazard analysis – at what frequencies do tsunamis occur and what is their size-frequency relationship?

6.1 Occurrence and Size

For the record and analysis of tsunami deposits below KS_{1907}, for each excavation we count the number of deposits between marker tephra and determine the approximate elevation above sea level and distance from shore of the excavation locale in that time (tephra) interval (Fig. S5). For some deposits, this excavation may be their limit and for others not (e.g., Fig. 9). We do not attempt to correlate sand layers from excavation to excavation (or profile to profile), though there are cases where it is possible. Rather, we count the maximum number of tsunami deposits between tephra, which is our indication of how many tsunami events have occurred.

Nat. Hazards Earth Syst. Sci. Discuss., https://doi.org/10.5194/nhess-2017-172
Manuscript under review for journal Nat. Hazards Earth Syst. Sci.
Discussion started: 20 June 2017

Natural Hazards and Earth System Sciences
Open Access
Discussions

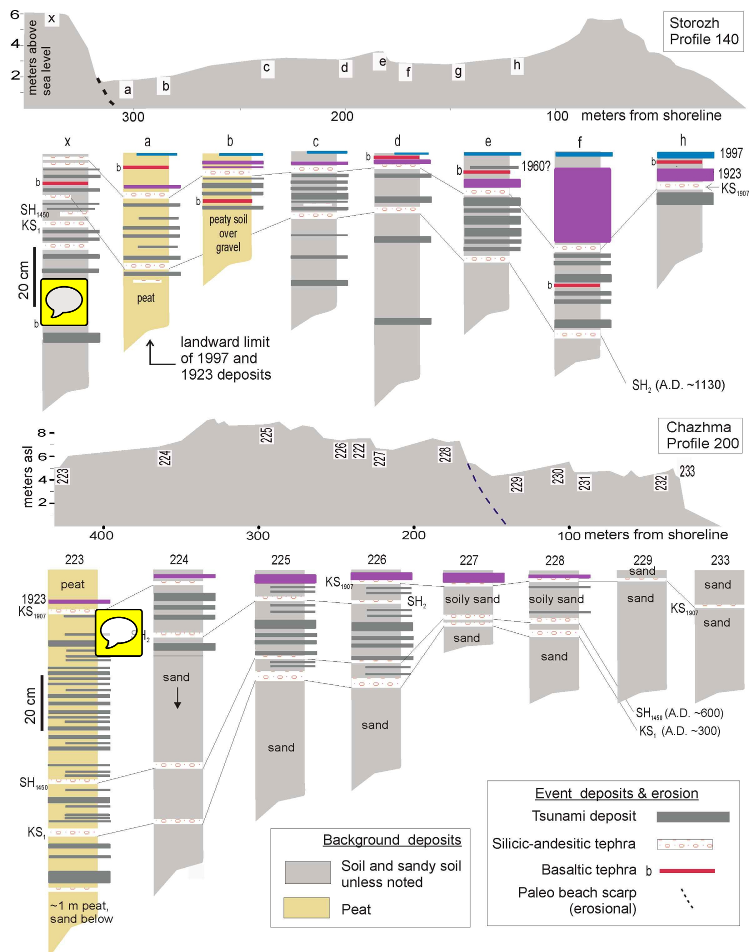

Figure 9. Example of two profiles that illustrate paleotsunami deposits used in analyses. Also see Figs. 4, 7, 8) **Storozh Profile 140 (top)**. Here we use this profile to illustrate an analysis of tsunami deposits between KS_{1907} and SH_2; note that the deposits thin landward, in general. In most excavations there are six tsunami deposits between KS_{1907} and SH_2; excavation "x" has only three. Thus all six tsunamis reached "a" but only three reached "x"; or, three of the six tsunamis only reached "a". All six tsunamis had to exceed the height of the shoreward beach ridge. **Chazhma Profile 200 (bottom).** As in Profile 110 (Fig. 8) this profile has undergone uplift through time. For sub-SH_2 deposits, the profile was reconstructed to 4 m lower and 150 m narrower. Sites 229-233 are young; the profile from 228 landward is older than KS_1 (A.D. ~300). Site 223 is not far from the modern Chazhma River and in the past some tsunamis may have flooded this site via the river, when the profile was lower. Sites 226 and 225 both have six deposits between SH_2 and SH_{1450}; no other excavation on this profile provides a good count in this interval, but these six deposits probably are in the record at 223, and 224 was simply too sandy to count all layers in this interval. SH_2 is not preserved (was not detected) in the peat excavation (223), but the 23 tsunami deposits in this excavation can be used in the overall count above KS_1. Excavations 223, 225 and 226 all preserve tsunami deposits between SH_{1450} and KS_1. In this interval the peat excavation (223) contains six deposits to the two in 225 and 226, for two possible reasons; first, peat is a better preserver/displayer of thin layers, and second, 223 is lower than 225 and 226 and at this time all were closer to shore. For the latter reason, 223 may have received tsunamis and their deposits directly from the river rather than over the beach ridge(s).

Nat. Hazards Earth Syst. Sci. Discuss., https://doi.org/10.5194/nhess-2017-172
Manuscript under review for journal Nat. Hazards Earth Syst. Sci.
Discussion started: 20 June 2017

Natural Hazards and Earth System Sciences
Open Access
Discussions

In order to summarize paleotsunami sizes, we determine sediment runup--or the highest point seaward, whichever is higher--and sediment inundation for tsunami deposits on each profile. For each tephra interval along each profile, there will be deposits at maximum distances and maximum elevations; the two measures are treated separately because tsunami deposits are not correlated (in fact, high runup is associated with shorter, steeper profiles and long inundation with low-relief profiles). For example, for the historical deposits, two points are plotted (Fig. 10) – their point of maximum inundation and their point of maximum runup, which are ~~on~~ usually on separate profiles.

A few of the paleo-events are comparable to Chile 1960 (Fig. 10), but most are likely from locally generated tsunamis because Chile 1960 was an outsized event and its deposits is not well represented on the profiles. The 1997 tsunami has dimensions similar to the majority of paleotsunamis as represented by sediment runup of on the order of 5-7 m (Fig. 10). The "1923" deposit, for which we do not know if related to February or April or both, is a "typical largest" event (Fig. 10). Recall that in these field sites there are few excavations at elevations of 10 m or more (Fig. S6), and that these higher elevations are on uplifted profiles, so we do not have a record of older paleotsunamis reaching such elevations, simply as an artefact of the data and analysis (Fig. S5). This issue is present also for paleo- inundation on prograding profiles, but is not such a strong artefact in this dataset. Overall, the number of deposits tends to decrease away from the coast and at higher elevations (density of points on Fig. 10), although there is a lot of scatter in the data, likely due to preservation and identification differences (e.g., Fig. 9).

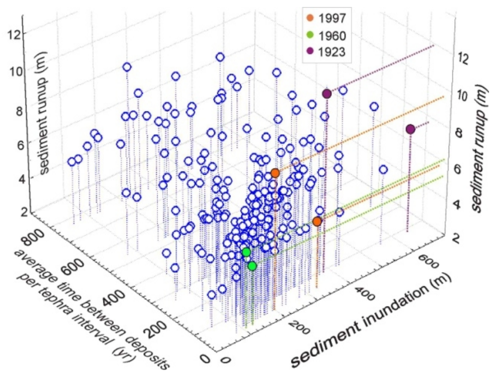

Figure 10. Three-dimensional diagram summarizing sediment runup and inundation for tsunami deposits, south Kamchatsky Bay, above KS$_1$ tephra (A.D. ~300, up through A.D. 2000) (from data plotted in Figs. S7 and S8). The three historical tsunami deposits are highlighted with their two points of maximum runup and maximum inundation, which do not coincide. For prehistoric events, we calculated (sediment) runup and inundation per tephra interval, with adjustments for changes through time in shoreline location and excavation elevation (see text and Fig. S5). The axis "average time between deposits" is biased by deposit counts and short time intervals but is shown here for general pattern.

6.2 Recurrence

To determine tsunami recurrence according to size, we consider all tsunami deposits above KS$_1$ (A.D. ~300) (Fig. 11). There are intermediate Shiveluch tephra layers between KS$_{1907}$ and KS$_1$ (Table 2), but their presence is not consistent enough to break down recurrence statistics, and the time intervals are relatively short relative to the number of events, so statistical analysis cannot be supported. For this exercise, we only use excavations now at or reconstructed to be more than 5 m above sea level or landward of a beach ridge (reconstructed to be) higher than 5 m. The grand total of the maximum number of events per each interval is 18 deposits, including

Nat. Hazards Earth Syst. Sci. Discuss., https://doi.org/10.5194/nhess-2017-172
Manuscript under review for journal Nat. Hazards Earth Syst. Sci.
Discussion started: 20 June 2017

Natural Hazards and Earth System Sciences
Open Access
Discussions

the historical cases. For each event, we determine a maximum sediment runup, that is, if there are four deposits between two marker tephra on a given profile, we determine the four highest points those deposits reach; e.g., two may reach 8.3 m and the other two only 7.2 m (all four reaching 7.2 m). We use reconstructed distances and elevations for each time interval below KS_{1907}. The maximum elevation is either sediment runup, h, or maximum elevation before sediment runup, H (as in Fig. 5), whichever is higher. Independent of the determined maximum elevation, we determine a maximum sediment inundation for each deposit in each tephra interval.

All 18 deposits reached elevations of 5 m (smaller not considered) and inland distances of 100 m, each factor with a recurrence interval of about 100 years (Fig. 11). Note again that runup and inundation are not paired; high runup commonly occurs on shorter, steeper profiles and long inundation on lower profiles. Tsunamis reaching an elevation of at least 7 m have a recurrence of ~200 years (Fig. 11). The largest reconstructed tsunamis as recorded by tsunami deposits have runup of 10 m or more and occur on average every 425 yr. Tsunamis with inundation of 600 m or more occur on average every ~570 yr.

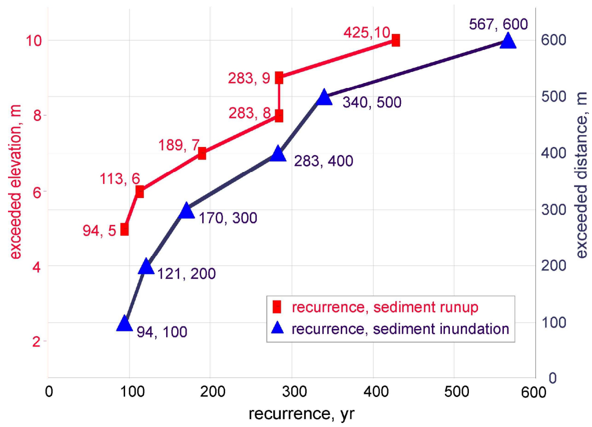

Figure 11. Tsunami (>5 m) recurrence for exceeded elevations (sediment runup) and exceeded distances from shoreline (sediment inundation) of tsunami deposits since KS_1 (A.D. ~300) in south Kamchatsky Bay. (For runup, integers of m are shown; for inundation, multiples of 100 m.) For example, tsunamis with runup of 8-9 m or more occur on average every 283 years. Tsunamis exceeding inundation of 500 m occur on average every 340 years. Recall that runup and inundation are not paired (see text).

7 Discussion and conclusions

7.1 Historical tsunamis

This work adds to the tsunami catalogue for 1997 Kronotsky and 1960 Chile, but not February or April 1923 Kamchatka events because we cannot differentiate the (two) 1923 deposits. The nearfield nature of the 1997 Kronotsky tsunami is significantly revised by this study of coastal profiles north of the Kronotsky Peninsula, adding substantial data to its catalogue. The 1997 tsunami reached runup heights of more than 9 m, averaging 6 m over about 60 km of coastline. As would be expected, tsunami heights (as indicated by deposits) and inundation distances are influenced by the coastal topography, with higher runups on steep profiles and higher inundation on lower-relief profiles. Data catalogues do not commonly provide topographic profiles, yet this information can be critical to understanding a tsunami and its generating source.

Based on deposits from 15 profiles and more than one hundred excavations, we conclude that the 1923 tsunami (February or April indeterminate) was larger than the December 1997 Kronotsky tsunami, but the summary and tabulated data (Fig. 6, Table 3) are tricky to interpret, with sediment inundation (L) being more indicative of tsunami size than runup (h) or highest point seaward of runup (H). On the basis of the total number of profiles exhibiting a deposit, "1923" is more extensive, but its average sediment runup (h) value is lower because the farthest point it reached on a number of profiles is actually lower than the points for 1997. Moreover, even though "1923" exceeded more of the high beach ridges seaward of the (sediment) runup point (H), the average of those is almost the same as for 1997 (Table 3). The most telling measurements distinguishing 1997 from "1923" are sediment inundation distances, with the average for "1923" almost twice that for 1997.

The 1952 tsunami deposit in southern Kamchatka (and the northern Kuril Islands) (MacInnes et al., 2010) reaches greater heights and inundation distances along its earthquake rupture zone than any of the historical tsunami deposits along the northern part of the Kamchatka subduction zone (this study; Pinegina, 2014). While this observation is not surprising given that 1952 was Mw 9.0 and the historical events to the north no larger than about Mw 8.5, the question to address is, can (does) the northern part of the subduction zone produce Mw 9 events, or does Kronotsky Cape represent an asperity that keeps ruptures shorter, as in 1923? For that, we must turn to the prehistoric record.

7.2 Implications for the 1997 Kronotsky earthquake rupture and the 1923 events

The sediment runup and inundation data reported here require a reevaluation of rupture source models for the 1997 Kronotsky earthquake; models which place most rupture energy to the south of or under the peninsula are not consistent with the tsunami data. The tsunami, rather than being unusually small for its generating earthquake's moment magnitude (Sohn, 1998), generated runup averaging 6 m over about 60 km of coastline, and 30 cm amplitude on the Hilo tide gage, requiring a "normal" offshore, subduction-zone rupture under a substantial depth of water. Some significant portion of that rupture must be under substantial water depth to produce the indicated tsunami north of Kronotsky Cape, while not generating as much runup on the Cape, or to the south. While part of the rupture could well have been under the Kronotsky Peninsula and the relatively shallow region directly offshore, deformation in deeper water east and north of the peninsula is needed.

We conclude that a rupture consistent with the mainshock and aftershock locations from Kamchatka's network are more reasonable than more westerly locations, e.g., in the ISC catalogue (Fig. 2, Table S2). This issue is illustrated by Hayes (2017) inversion, which takes the NEIC hypocentral location (Table S2) to start and, while his inversion results in most slip to the north (Fig. S9), locates that slip under the peninsula, where it cannot generate a tsunami.

The northern part of the Kamchatka subduction zone ruptured in two large events in February 1923 and April 1923 (Fig. 1), and our study requires that a substantial portion of the energy released by the 1997 Kronotsky earthquake was generated in a seismic gap between those earthquakes (Fig. 1), as originally recognized by Fedotov et al. (1998) and predicted by his group's earlier work. The Kronotsky Peninsula lies landward of the (subducting) Emperor Seamount chain, which has been postulated to generate an asperity and is characterized by a relatively strong positive gravity anomaly (e.g., Bürgmann et al., 2005, Llenos and McGuire, 2007; Bassett and Watts, 2015) (Fig. S9). That asperity may well keep the northern Kamchatka subduction zone from generating (Mw 9) 1952-scale Kamchatka earthquakes, but it does rupture, as required by the tsunami data presented herein.

7.3 Paleotsunami results – implications for tectonic studies and hazard analyses

Southern Kamchatsky Bay has a relatively short but well-preserved record of paleotsunami deposits which can be calibrated with the historical record. Combined with the record in north Kamchatsky Bay (Pinegina et al., 2012) (the central bay is characterized by cliffs), the pattern of runup and inundation in the prehistoric record for the last 1700 years does not diverge from the 20th century record. Compared with southern Kamchatka, the region where Mw 9-scale events occurred in 1952 and 1737, the northern subduction zone has generated smaller and less extensive tsunamis, in agreement with analyses of Bürgmann et al. (2005) for the modern and Pinegina (2014) for the prehistoric record.

A robust, 1700-year-long record may be sufficient to generate a probabilistic hazard analysis that can be used for both local and far-field hazard studies, and not only for tsunami recurrence statistics, but also for recurrence statistics that include tsunami size. Reconstructing paleo- runup and paleo- inundation requires, and is thus limited by, accurate reconstructions of past shoreline locations and past (relative) sea levels. Coastlines with well-established marker tephra enable such reconstructions.

As are seismologists, paleoseismologists are cautioned by the lessons of the 11 March 2011 Tohoku earthquake and tsunami to qualify our generalizations. Characterizing subduction-zone behavior and quantifying its hazards are goals which we will only ever accomplish imperfectly.

Supplement link (will be included by Copernicus) – see supplemental material

Author contribution – we contributed equally and together

Competing interests -- none

Acknowledgments

Field research was supported by grants from the Russian Foundation for Fundamental Research (00-05-64697-a to T.K. Pinegina), the National Geographic Foundation to Vera Ponomareva, and the U.S. National Science Foundation (EAR 9903341 to J. Bourgeois). Research and manuscript preparation were supported by RFBR grant 15-05-02651- to T. Pinegina and a U.S. Fulbright Foundation award to J. Bourgeois, which supported her visit to the Institute of Volcanology and Seismology, winter/spring of 2017.

We thank Vera Ponomareva for field advice and discussions regarding tephra stratigraphy and analysis; Alexander Lander for discussions concerning the nature of the 1997 Kronotsky earthquake; Alexander Gusev for discussions regarding the 1997 and earlier large earthquakes on Kamchatka; Vasily Titov for insights into the 1997 Kronotsky tsunami; and Vadim Saltykov for his helpful recommendations about statistical analyses of tsunami recurrence. We are grateful to Alexander Storcheus (deceased), Leonid Kotenko, Ivan Storcheus and Edward Cranswick for their field assistance. Roland Bürgmann, Andrea Llenos and Gavin Hayes offered helpful insights into their source models for 1997 Kronotsky.

References

Ammon, C. J., Kanamori, H. and Lay, T.: A great earthquake doublet and seismic stress transfer cycle in the central Kuril islands, Nature 451.7178, 561-565, doi:10.1038/nature06521, 2008.

Balakina, L.M.: The October 4, 1994 Shikotan and December 5, 1997 Kronotsky earthquakes and their strongest aftershocks as regular manifestations of the tectonic process in the Kuril-Kamchatka seismogenic zone, Izvestiya - Russian Academy of Sciences, Physics of the Solid Earth, 36, 903-918, 2000.

Bassett, D. and Watts, A. B.: Gravity anomalies, crustal structure, and seismicity at subduction zones: 1. Seafloor roughness and subducting relief, Geochemistry, Geophysics, Geosystems, 16, 1508-1540, doi/10.1002/2014GC005684, 2015.

Bourgeois, J.: Geologic effects and records of tsunamis, Chapter 3 in The Sea, volume 15, Tsunamis, Harvard University Press, 55-91, 2009.

Bourgeois, J., and Titov, V.V.: A Fresh Look at the 1997 Kronosky Tsunami, Transactions of the European Geophysical Society, Abstracts, 2001.

Bourgeois, J., Pinegina, T., Ponomareva, V. and Zaretskaia, N.: Holocene tsunamis in the southwestern Bering Sea, Russian Far East, and their tectonic implications, Geological Society of America Bulletin, 118, 449-463, doi: 10.1130/B25726.1, 2006.

Braitseva, O.A., Ponomareva, V.V., Sulerzhitsky, L.D., Melekestsev, I.V. and Bailey, J.: Holocene key-marker tephra layers in Kamchatka, Russia, Quaternary research, 47, 125-139, doi.org/10.1006/qres.1996.1876, 1997.

Bürgmann, R., Kogan, M.G., Levin, V.E., Scholz, C.H., King, R.W. and Steblov, G.M.: Rapid aseismic moment release following the 5 December, 1997 Kronotsky, Kamchatka, earthquake, Geophys. Res. Lett., 28, 1331-1334, doi: 10.1029/2000GL012350, 2001.

Bürgmann, R., Kogan, M.G., Steblov, G.M., Hilley, G., Levin, V.E. and Apel, E.: Interseismic coupling and asperity distribution along the Kamchatka subduction zone, J. Geophys. Res., 110, B07405, doi/10.1029/2005JB003648, 2005.

Fedotov, S.A., Chernyshev, S.D., Matviyenko, Y.D., and Zharinov, N.A.: Prediction of Kronotskoye earthquake of December 5, 1997, M = 7.8-7.9, Kamchatka, and its strong aftershocks with M > or = 6, Volcanology and Seismology, 6, 3-16, 1998, [in Russian].

Godzikovskaya, A.A.: Summary of macroseismic information on Kamchatka earthquakes (Pre-instrumental and early instrumental observation period), Moskow – Petropavlovsk-Kamchatsky, 134 pp., 2010 [in Russian].

Gordeev, E.I., Ivanov, B.V. and Vikulin, A.V. (eds.): Kronotskoye earthquake of December 5, 1997 on Kamchatka, Petropavlovsk-Kamchatsky, Kamchatkan State Academy of Fishing Marine, 294 pp., 1998, [in Russian with English abstracts and figure captions].

Gordeev, E.I., Gusev, A.A., Levin, V.E., Bakhtiarov, V.F., Pavlov, V.M., Chebrov, V.N. and Kasahara, M.: Preliminary analysis of deformation of the Eurasia-Pacific-North America plate junction from GPS data, Geophys. J. Int., 147, 189-198, doi: https://doi.org/10.1046/j.0956-540x.2001.01515.x, 2001.

Nat. Hazards Earth Syst. Sci. Discuss., https://doi.org/10.5194/nhess-2017-172
Manuscript under review for journal Nat. Hazards Earth Syst. Sci.
Discussion started: 20 June 2017

Natural Hazards and Earth System Sciences
Open Access
Discussions

Gusev, A.A., Levina, V.I., Saltykov, V.A., and Gordeev, E.I.: Large Kronotskoye earthquake of Dec. 5, 1997: basic data, seismicity of the epicentral zone, source mechanism, macroseismic effects, in Gordeev et al., eds., 32-54, 1998 [In Russian with English abstract and figure captions].

Gusev, A. A.: The schematic map of the source zones of large Kamchatka earthquakes of the instrumental epoch: in Complex seismological and geophysical researches of Kamchatka. To 25th Anniversary of Kamchatkan Experimental & Methodical Seismological Department, Ed. by Gordeev E.I., Chebrov V.N., Petropavlovsk-Kamchatsky, 445 pp., 2004.

Gusev, A.A. and Shumilina, L.S.: Recurrence of Kamchatka strong earthquakes on a scale of moment magnitudes, Izvestiya, Physics of the Solid Earth, 40, 206-215, 2004.

Hayes, Gavin P.: The finite, kinematic rupture properties of great-sized earthquakes since 1990, Earth and Planetary Science Letters, 468, 94-100, doi: https://doi.org/10.1016/j.epsl.2017.04.003, 2017.

Kuzin, I.P., Levina, V.I., and Flenov, A.B.: Body wave velocity distribution in the Benioff zone of central Kamchatka during aftershocks of the Kronotskii earthquake of 1997 (M = 7.9), J. Volcanology & Seismology, 1, 175-184, doi: 10.1134/S0742046307030037, 2007.

Kyle, P. R., Ponomareva, V. V., and Schluep, R. R.: Geochemical characterization of marker tephra layers from major Holocene eruptions, Kamchatka Peninsula, Russia, International Geology Review, 53, 1059-1097, http://dx.doi.org/10.1080/00206810903442162, 2011.

Leonov, V.L.: Ground ruptures, landslides and rockfalls caused by the earthquake on December 5, 1997 at the sea-board of Kronotsky Peninsula: in Gordeev et al., eds., 240-246, 1998.

Levina, V. I., Lander, A. V., Mityushkina, S. V., and Chebrova, A. Y. The seismicity of the Kamchatka region: 1962–2011, Journal of Volcanology and Seismology, 7, 37-57, doi:10.1134/S0742046313010053, 2013.

Llenos, A. L., and McGuire, J. J.: Influence of fore-arc structure on the extent of great subduction zone earthquakes, Journal of Geophysical Research: Solid Earth, 112, B09301, doi:10.1029/2007JB004944, 2007.

Liu, P. L. F.: Tsunami modeling: propagation, The Sea, 15, 295-319, 2009.

MacInnes, B. T., Pinegina, T. K. Bourgeois, J, Razhigaeva, N, G., Kaistrenko, V. M., and Kravchunovskaya, E. A.: Field survey and geological effects of the 15 November 2006 Kuril tsunami in the middle Kuril Islands: In Tsunami Science Four Years after the 2004 Indian Ocean Tsunami, Birkhäuser Basel, 9-36, doi 10.1007/s00024-008-0428-3, 2009.

MacInnes, B.T., Weiss, R., Bourgeois, J. and Pinegina, T.K.: Slip distribution of the 1952 Kamchatka great earthquake based on near-field tsunami deposits and historical records, Bulletin of the Seismological Society of America, 100, 1695-1709, doi: 10.1785/0120090376, 2010.

MacInnes, B., Kravchunovskaya, E., Pinegina, T., and Bourgeois, J. Paleotsunamis from the central Kuril Islands segment of the Japan-Kuril-Kamchatka subduction zone, Quaternary Research, 86, 54-66, https://doi.org/10.1016/j.yqres.2016.03.005, 2016.

Martin, M. E., Weiss, R., Bourgeois, J., Pinegina, T. K, Houston, H. and Titov, V. V. Combining constraints from tsunami modeling and sedimentology to untangle the 1969 Ozernoi and 1971 Kamchatskii tsunamis, Geophys. Res. Lett., 35, L01610, doi:10.1029/2007GL032349, 2008.

Nat. Hazards Earth Syst. Sci. Discuss., https://doi.org/10.5194/nhess-2017-172
Manuscript under review for journal Nat. Hazards Earth Syst. Sci.
Discussion started: 20 June 2017

Natural Hazards and Earth System Sciences
Open Access
Discussions

Melekestsev, I.V, Braitseva, O.A., Erlikh, E.N., Shantser, A.E., Chelebaeva, A.I., Lupikina E.G., Egorova, I.A., Kozhemyaka, N.N.: Kamchatka, Komandor and Kurile Islands, Moskow, Nauka, 439 pp., 1974 [in Russian].

Nanayama, F., Furukawa, R., Shigeno, K., Makino, A., Soeda, Y. and Igarashi, Y.: Nine unusually large tsunami deposits from the past 4000 years at Kiritappu marsh along the southern Kuril Trench, Sedimentary Geology, 200, 275-294, https://doi.org/10.1016/j.sedgeo.2007.01.008, 2007.

NCEI, National Centers for Environmental Information (formerly NGDC), Natural Hazards Data, Images and Education, Tsunami and Earthquake databases: https://www.ngdc.noaa.gov/hazard/hazards.shtml

Okal, E.A. and Synolakis, C.E.: Source discriminants for near-field tsunamis, Geophysical Journal International, 158, 899-912, DOI: https://doi.org/10.1111/j.1365-246X.2004.02347.x, 2004.

Petukhin, A.G., Dontsov, O.V., Kozlov, V.N., and Sinitsyn, V.I.: Preliminary analysis of strong ground-motion records of the Kronotskoye earthquake of December 5, 1997 (Mw = 7.9): in Gordeev et al., eds., 247-256, 1998, [In Russian with English abstract and figure captions].

Pinegina T. K.: Time-space distribution of tsunamigenic earthquakes along the Pacific and Bering coasts of Kamchatka: insight from paleotsunami deposits, Doctor of Geological Science dissertation, Institute of Oceanology RAS, Moscow, 235 pp., 2014 [in Russian].

Pinegina, T. K., Kozhurin, A. I., Ponomareva, V. V.: Seismic and tsunami hazard assessment for Ust-Kamchatsk settlement, Kamchatka, based on paleoseismological data, Bulletin of Kamchatka regional association "Educational-scientific center". Earth sciences. 1, 138-159, 2012 [in Russian with English abstract].

Pinegina, T.K., Bourgeois, J., Kravchunovskaya, E.A., Lander, A.V., Arcos, M.E., Pedoja, K. and MacInnes, B.T.: A nexus of plate interaction: Vertical deformation of Holocene wave-built terraces on the Kamchatsky Peninsula (Kamchatka, Russia), Geological Society of America Bulletin, 125, 1554-1568, doi: 10.1130/B30793.1, 2013.

Ponomareva, V., Portnyagin, M., Pendea, I.F., Zelenin, E., Bourgeois, J., Pinegina, T., and Kozhurin A. A.: A full Holocene tephrochronology for the Kamchatsky Peninsula region: applications from Kamchatka to North America, Quaternary Science Reviews, 2017 [in press].

Slavina, L.B., Pivovarova, N.B. and Levina, V.I.: A study in the velocity structure of December 5, 1997, Mw = 7.8 Kronotskii rupture zone, Kamchatka, J. Volcanology & Seismology, 1, 254-262, doi:10.1134/S0742046307040045, 2007.

Sohn, S.W.: The 1997 Kamchatka earthquake. Individual Studies by Participants at the International Institute of Seismology and Earthquake Engineering, Tokyo, International, 34, 91-99,1998.

Song, T. R. A. and Simons, M.: Large trench-parallel gravity variations predict seismogenic behavior in subduction zones, Science, 301, 630-633, DOI: 10.1126/science.1085557, 2003.

Zayakin, Yu. A. and Luchinina, A.A.: Catalogue tsunamis on Kamchatka, Obninsk: Vniigmi-Mtsd, 51pp., 1987, [Booklet in Russian].

Zayakin, Yu. A. and Pinegina, T.K.: Tsunami in Kamchatka on December 5, 1997: in Gordeev et al., eds., 257-263, 1998, [In Russian with English abstract and figure captions].

Nat. Hazards Earth Syst. Sci. Discuss., https://doi.org/10.5194/nhess-2017-172
Manuscript under review for journal Nat. Hazards Earth Syst. Sci.
Discussion started: 20 June 2017

Natural Hazards and Earth System Sciences
Open Access
Discussions

Zobin, V.M. and Levina, V.I.: The rupture process of the Mw 7.8 Cape Kronotsky, Kamchatka, earthquake of 5 December 1997 and its relationship to foreshocks and aftershocks, Bull. Seis. Soc. Am., 91, 1619-1628, doi: 10.1785/0119990116, 2001.

Supplement to accompany J. Bourgeois & T.K. Pinegina

1997 Kronotsky earthquake and tsunami and their predecessors, Kamchatka, Russia

Earthquake and tsunami data

This supplement includes a reproduction of the original figure by Gusev (2004) of source regions for large Kamchatka earthquakes since 1899 (Fig. S1). In our paper, we use a revised version of this figure and discuss the bases for our suggested revisions.

Tsunamis have arrived to Kamchatka not only from local earthquakes but also from other regions, of which Kamchatka is particularly susceptible to tsunamis from Chile; Kamchatka is shadowed (protected) from non-local tsunamis originating in the North Pacific (Table S1; localities on Fig. S2). In order to interpret 20th century tsunami deposits in our field sites, we use these data to evaluate the possibility that at least one of the deposits is from a far-field event, Chile 1960.

Table S2 provides a summary of different researchers' assignments of moment magnitude, locations of mainshock epicenter and hypocenter, and centroid determinations for the December 1997 Kronotsky earthquake. There are some significant differences, which we discuss in our paper in terms of our documented evidence for tsunami runup averaging about 6 m along the coast north of Kronotsky Peninsula.

Figure S3 is a version of a previously published photo and sketch interpretation of 1997 Kronotsky tsunami effects on Kronotsky Cape (Pinegina et al., 2003).

The magnitudes of tsunamigenic and other large earthquakes originating along the Kamchatka subduction zone (and to its north) have been evaluated by Gusev and Shumilina (2004), with some suggested revisions to other catalogues (Table S3). One indicator of moment magnitude of earthquakes originating along the Kuril-Kamchatka subduction zone is their tide-gage amplitude in Hilo, Hawaii, as shown in Table S3 for all historical earthquakes and in Figure S4 for events with a tide-gage record in Hilo.

In A.D. 1923, there were two tsunamigenic earthquakes along the northern Kamchatka subduction zone. Table S4 is a compilation of information about those two tsunamis, which both affected Kamchatsky Bay. These observations and data help us evaluate which of these two tsunamis may have affected our field area in south Kamchatsky Bay.

Methodology for reconstructing paleoshorelines (Figure S5)

Many profiles show evidence of changes through time in beach-plain width and in surface elevation relative to sea level; that is, the shoreward, older parts of profiles are higher or lower than the seaward parts (Figure S5). Ideally, a reconstruction of the prehistoric coast and hence of paleotsunami size (runup and inundation as approximated by deposit extent) will include an estimate of horizontal shifts of shoreline location for paleo-inundation and an approximation of change in relative sea level for paleo- runup. We use tephra stratigraphy (as in Pinegina et al., 2013; MacInnes et al., 2016) and tephra mapping along profiles in order to reconstruct paleo-profiles. The reconstruction of the south Kamchatsky Bay profiles and their paleotsunamis was first performed and reported by Pinegina (2014).

Horizontal changes (Figure S5). We use the methods of Pinegina et al. (2013; also see MacInnes et al., 2016). These methods make an assumption that no widespread erosion has occurred, which is reasonable for the last 2000 years in south Kamchatsky Bay, but is a potential source of error. South Kamchatsky Bay profiles all indicate net progradation during the time interval examined. A tephra deposit is typically preserved in stratigraphy inland from the first dense vegetation (point *dv* on Figure S5) landward of the active (sandy) beach. Therefore, the seaward extent of a tephra in the stratigraphy (*dv1* or *dv3* in Figure S5) indicates the *dv* position at the time of eruption and ash deposition. Assuming today's active beach width is representative of the past, we estimate the shoreline position at time "tephra x" to be the paleo *dv(x)* plus the modern active beach width. In general, our paleo- inundation estimates are minima because even though the beach-ridge plains are net progradational, short-lived periods of erosion can remove some of the accumulated coastal width. A general limitation to paleotsunami inundation reconstruction on a prograding shoreline is that estimates of maximum paleo- inundation will decrease back in time as the reconstructed beach plain width decreases. On the other hand, past erosion, which cannot be reconstructed, will result in an underestimate of beach plain width.

Vertical changes (Figure S5)**.** In order to determine the change in land level relative to the sea, in each excavation we identify an elevation tied to sea level, for which we also use the point of the first growth of dense vegetation (*dv*, Figure S5). We measure and mark this point on our modern profiles and associate this point in excavations with good preservation of volcanic ash layers (tephra). The limit of dense vegetation approximates the swash limit and storm high tide, seaward of which tephra will rarely be preserved. Dense vegetation (primarily dune grass, *Elymus* sp.) grows only on the part of the profile that is rarely affected by storms, except for some washover, and thus soil-tephra cover begins to form on these surfaces. Net uplift or subsidence is the difference between the modern *dv* elevation and the paleo *dv* elevation (Figure S5). A general limit to paleotsunami runup estimates for the case of uplifting coastlines is that maximum paleo- runup will decrease back in time as the reconstructions bring paleo- profiles downward.

Historical and paleotsunami data, including excavation elevations and distances from shoreline

Herein we summarize graphically the data on which our paleotsunami analysis is based. These data were first synthesized by Pinegina (2014) for many localities along the Pacific coast of Kamchatka. In this supplement, we include data from Ust-Kamchatsk (Pinegina et al. 2012; Pinegina 2014) because it is within (at the north end of) Kamchatsky Bay (Fig. S2).

The distribution of elevations (meters above sea level) and distances (meters from modern shoreline) of excavations in the field area, southern Kamchatsky Bay, are shown in Figure S6. We use these distances and elevations for reconstructing tsunami sediment runup and inundation for 20th century tsunami deposits (Fig. S7). For south Kamchatsky Bay, the maximum profile width is less than 800 m; in north Kamchatsky Bay, distances reach about 1.8 km (Figs. S7, S8).

The elevation and distance of tsunami deposits above KS_{1907}, including data from the Ust-Kamchatsk area, north Kamchatsky Bay, are shown in Figure S7. Some excavations contain no deposits above KS_{1907}. The deposit that is present in the most excavations we interpret as from 1923; the second-most extensive deposit is from 1997. Rarely there is a third deposit between the other two, which we assign to 1960 Chile.

The number of paleotsunami deposits per tephra interval for three intervals below KS_{1907} are shown in Figure S8, which includes data from north Kamchatsky Bay near Ust-Kamchatsk. For each interval, the elevation and distance from shoreline of each excavation is reconstructed using methods as in Figure S5.

Locations of the 5 December 1997 Kronotsky earthquake rupture, according to different studies

Our tsunami-deposit study has implications for the rupture zone of the 1997 Kronotsky earthquake. Figure S9 is a compilation of several different models for the location of this rupture zone, from previously published work.

Table S1. HISTORICAL TSUNAMIS AFFECTING (or possibly affecting) THE KAMCHATSKIY BAY COAST OF KAMCHATKA*

EARTHQUAKE PARAMETERS			RECORDS OF TSUNAMI RUNUP (*tide gage records in italics*) in meters									
			Locations South to North Olga Bay to Bering Island								MAX KAM	Hilo, HI
Date (local)	Source region	Mw	Olga Bay	Kron. Cape	CHAZHMA ADR-BIST	Shuber-tovo	south of U-K	*U-K tide gage*	Kamch River	Bering I. (south)		
5-Dec-97	Kronotskiy Peninsula	7.8/7.9^	0.5-1	1.5	this paper			*not working*		*incompl record*	this paper	*0.24*
8-May-86	Andreanof Islands#	8						*0.04*		*0.09*	*0.09*	*0.28*
4-Mar-85	Chile	7.7						*0.03*				*0.77*
28-Dec-84	Kamchatsky Strait	7						*0.02*		*0.17*		
18-Aug-83	Kamchatsky Bay	6.8						*0.02*				
15-Dec-71	Commander Is.	7.8^						*0.47*				*0.10*
23-Nov-69	Bering Sea	7.7						*0.2*			10-15	*0.10*
04-Feb-65	w. Aleutians	8.7	only recorded on Petropavlovsk tide gage								*0.08*	*0.30*
28-Mar-64	Alaskan Peninsula	9.2	only recorded on Petropavlovsk tide gage								*0.06*	~3
24-May-60	Chile	9.5	4				3	*0.8*	3-4	3-3.5	7	~10
05-Nov-52	s. Kamchatka	9	10-13			0.5-1		*0.1*		2	10-15	*1.1*
02-Apr-46	Aleutians	8.1	no record on Kamchatka 0.1-0.2 in northern Japan, max 1.1 in Japan								—	~9
14-Apr-23	Kamchatskiy Bay	7.3/8.2^					20-30		11	4	20-30	*0.30*
04-Feb-23	Kronotskiy Bay	8.5^	4-5 km up river		4-5 km up Chazhma R.				3		6-8	6.10
17 May 1841	s. Kamchatka	9^									15	4.6
August 1792	Avachinsky Bay to n. Kamchatsky Bay	8.25**										
15 Apr 1791	Kamchatskiy Bay	(7.5)^							effects 7 km upstream			—
4 Nov 1737	N Kamchatskiy Bay	(7.8)^										
17 Oct 1737	s. Kamchatka	9.2^									>30?	—

*Primary sources: Zayakin and Luchinina, 1987; NEIC (formerly NGDC) Natural Hazards Data, online

^Kamchatka Mw's from Gusev and Shumilina, 2004; G&S 8.2 for 14Apr23 is based on tsunami; see text discussion

#Andreanof Islands, 1996, 7.9, 1957, 8.6, no catalogue observations for Russia

**Ms from Zayakin & Luchinina

Table S2. Epicentral locations, centroids and moment magnitudes for the 5 December 1997 Kronotsky earthquake (ISC* Event 1056468 "Near east coast of Kamchatka Peninsula")

Origin of analysis	ISC*origin ID	Lat °N	Long °E	Moment/Mw	Additional information
Epicenter/Mainshock^					
KEMSD GS RAS		54.95	163.23		Gusev et al. 1998, Luneva&Lee 2003
Zobin& Levina 2001; Slavina et al. 2007		54.64	162.58		Kamchatka network catalogue; S&al 162.55
KRSC reported in ISC database	2296136	54.64	162.55		ISC KRSC = KEMSD
ISC--International Seismological Centre	1056468	54.8043	162.0069		accessed online 13 Mar 2017
Engdahl and Villsenor 2002	2329842	54.797	162.003		ISC-CENT--Centennial Catalogue
EHB — reported in ISC online	9258772	54.792	162.001		ISC — Engdahl, vonderHilst & Buland, 1998
NAO — reported in ISC online	2296140	55	162		ISC — NORSAR, Norway
EIDC — Arlington, VA	2296135	54.8523	161.9921		ISC—Experim. (GSETT3) Internatl Data Ctr
BJI — China	2296137	54.82	161.90		ISC — China Earthquake Administration
Centroid/Moment Tensor solutions & models					
Geophys Survey Russian Academy Sci.	2296139	54.881	161.947	$2.2x10^{20}$Nm	ISC — MOS, Obninsk
NEIC, Golden, CO [USGS]	2296138, 5159529	54.841	162.035	$4.1x10^{20}$Nm	ISC; National Earthquake Information Center
Global CMT [formerly Harvard]	2296141	54.31	161.91	7.8	ISC - HRVD, Global GMT #120597C
Harvard CMT early		54.08	162.29	7.9	reported in Gusev et al., 1998
Sohn, 1998		54.8	162	uses $2.5x10^{20}$Nm	model from tsunami analysis; location approx.
Burgmann et al. 2001		$54.19^{\#}$	$162.57^{\#}$	uses $3.8x10^{20}$Nm	acos model based on GPS data
Burgmann et al. 2001		$54.23^{\#}$	$162.33^{\#}$	uses $4.1x10^{20}$Nm	bcos model based on GPS data

*ISC = International Seismological Centre, *On-line Bulletin* , http://www.isc.ac.uk, Internatl. Seismol. Cent., Thatcham, United Kingdom, 2014; last accessed 20 March 2017

^Ordered by longitude, easternmost to westernmost

#Latitude and longitude refer to the center of the upper dislocation edge of the modeled centroid

Table S3: Historical tsunamigenic events in the Kuril-Kamchatka region and their record in Hilo, Hawaii

Date (young to old)			Location epicenter/rupture		Earthquake		Tsunami runup/tide			
Year	Mo	Day	Latitude °N	Region	M NCEI	Mw^	Runup max m	*Hilo tide* m	Hilo runup m	COMMENTS
2009	1	15	46.857	Central Kuril Is.	7.4	~	*	*0*		0.11 m tide gage Severo Kurilsk
2007	1	13	46.243	Central Kuril Is.	8	~	6-20**	*0.11*		outer rise event
2006	11	15	46.592	Central Kuril Is.	8.3	~	6-20**	*0.475*		
1997	12	5	54.88	Kamchatka	7.8	7.9	(9)	*0.24*		(runup max from deposits)
1995	12	3	44.663	S. Kuril Is.	7.9	~	*	*0.228*		
1994	10	4	43.773	Shikotan Is.	8.3	~	10.4	*0.16*		outer rise event
1993	6	8	51.25	S. Kamchatka	7.5	7.5	*	*0.06*		
1971	12	15	55.91	N. Kamchatka	7.8	7.8	(13)	*0.1*		0.47 on Ust' Kamch. tide gage; (runup max from deposits)
1969	11	22	57.8	N. Kamchatka	7.7	7.7	15	*0.1*		
1963	10	13	44.81	S. Kuril Is.	8.5	~	4.5	*0.4*		
1963	10	20	44.1	S. Kuril Is.	6.7	~	15	*0.1*		
1959	5	4	53.9	Kamchatka	8.2	8	1.5-2	*0.1* [#]		
1958	11	6	44.53	S. Kuril Is.	8.3	~	5	*0.2*		limited nearfield obs, 5 m on Shikotan
1958	11	12	44.2	S. Kuril Is.	7	~	1	*0.1*		
1952	11	4	52.3	Kamchatka-Kuril	9	9	(20)	*1.1*	3.4	(runup max from deposits)
1933	1	8	49.12	N. Kuril Is.	na	na	9	*0*		Kharimkotan landslide
1927	12	28	53.8	Kamchatka	7.3	7.5	*	*0.1*		
1923	4	13	55.4	N. Kamchatka	7.3	8.2	14	*0.3*		
1923	2	2	52.5	Kamchatka	8.3	8.5	8		6.1	
1918	9	7	45.5	S. Kuril Is.	8.2	~	12		1.5	
1917	1	30	55.2	N. Kamchatka		8	*			no tsunami; strike-slip event, Steller f.z.
1841	5	17	52.5	Kamchatka	8.4	9	15		4.6	
1737	10	17	50.5	S. Kamchatka		9.2	30?			
1737	11	4	55.5	N. Kamchatka		7.8	*			

Primary sources: Zayakin and Luchinina, 1987; NCEI Tsunami database

*no nearfield data

^from Gusev & Shumilina, 2004

[#]1959 measurement is from Honolulu

**2006 and 2007 runup could not be definitely distinguished in post-tsunami survey

Table S4. Comparison of measurements and observations, 1923 Kamchatka tsunamis

Observation locality	Latitude	Longitude	3 Feb 1923 Runup (m)	type	13 April 1923 Runup (m)	type
Bering Island, Commander Islands	55.20	166.01			4	1
Kamchatka Pacific coast, north to south						
Dembi Spit area, east Ust Kamchatsk	56.22	162.52			11	1
Kamchatka River	56.25	162.44			broke ice 7 km upriver	1
Tsutsumi fish plant	55.176	162.313	damaged cabin on first ridge*	1	4 km inundation** ext. damage	1
First River, north central Kamch Bay	56.05	162.05			20	1
Chazhma River, south Kamch Bay	55.06	161.82	4-5 km upriver	1		
Semyachik, central Kronotsky Bay	54.12	159.98	6	1		
Kolygir Bay, Shipunsky Peninsula	53.42	159.85	8	1		
Ostrovnoye, north Avachinsky Bay	53.25	159.57	obs	1		
Nalychevo R. north Avachinsky Bay	53.16	159.24	obs	1		
Khalaktirka, central Avachinsky Bay	52.98	158.83	8.4^	^		
Avachinsky Gulf (interior)	52.97	158.50	obs	1		
Japan Pacific coast, north to south						
Hanasaki, Hokkaido	43.278	145.568	*0.23*	*2*	*0.07*	*2*
Ayukawa, Miyagi, Japan	38.300	141.500	*0.33*	*2*	*0.17*	*2*
Kushimoto, Wakayama, Japan	33.467	135.783	*0.5*	*2*		
Hososhima, Miyazaki, Japan	32.433	131.667	*0.2*	*2*		
Pacific islands						
Hilo, Hawaii, HI, USA	19.733	-155.067	6.1	1	*0.3*	*2*
Kahului, Maui, HI, USA	20.895	-156.477	3.5	1		
Honolulu, Oahu, HI, USA	21.307	-157.867	*0.9*	*2*	*0.2*	*2*
Haleiva, Oahu, HI, USA	21.593	-158.106	3.7	1		
Apia, Upolu Is, Samoa	-13.827	-171.761	obs	*2*		
West coast North America. north to south						
Tofino, BC, Canada	49.153	-125.913	*0.14*	*2*	*0.08*	*2*
San Francisco, CA, USA	37.807	-122.465	*0.1*	*2*	*0.15*	*2*
Santa Cruz, CA, USA	36.970	-122.020	obs	1		
Los Angeles, CA, USA	33.717	-118.267	obs	1		
San Diego, CA, USA	32.715	-117.174	*0.2*	*2*	*0.1*	*2*

Primary source: for Kamchatka: Zayakin and Luchinina; remainder: NCEI catalogue

Type: 1 = runup, elevation above sea level; *2 = tide gage amplitude*

*first beach ridge ~3.5 m above sea level; second ~4 m asl (profile in Pinegina et al., 2014)

**inundation may have been via river to lagoonal areas between ridges; sediment inundation 1 km (Pinegina et al., 2012)

^based on deposits, Pinegina and Bazanova, 2016

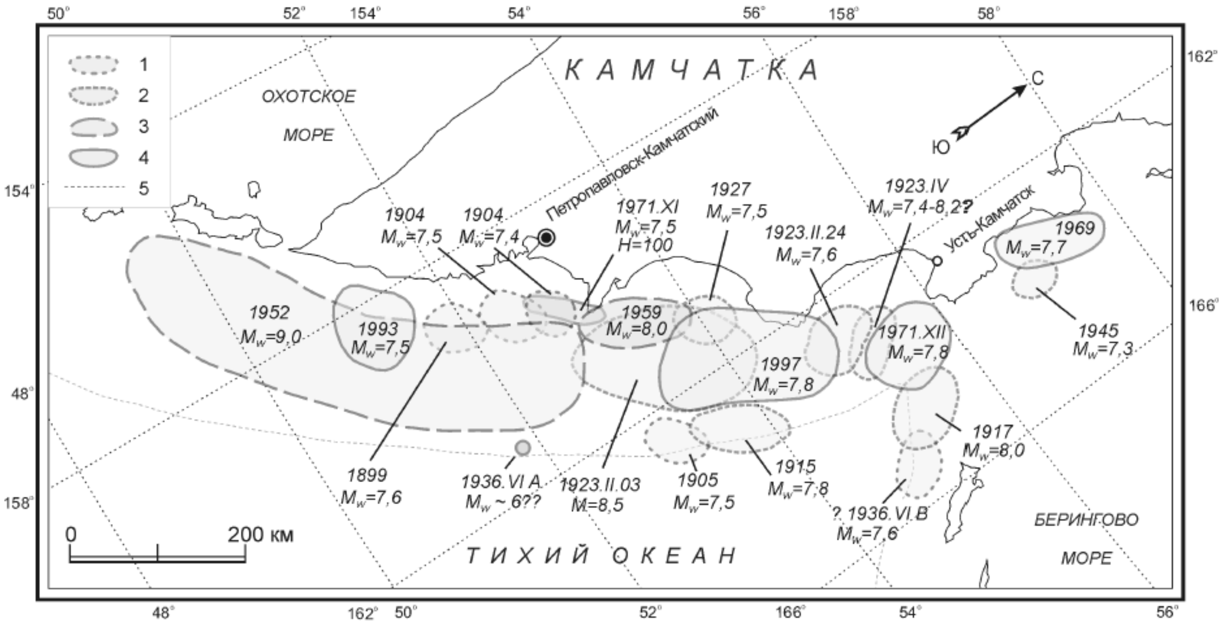

Рис. 1. Новый вариант расположения очаговых зон землетрясений Камчатки за 1899-2003 гг.

Figure S1. Original figure from which we make comments and suggested revisions in the text (Gusev, 2004; used with permission) Translated caption: "New version (of) source location zones of Kamchatka earthquakes 1899 to 2003." Also see Gusev and Shumilina (2004).

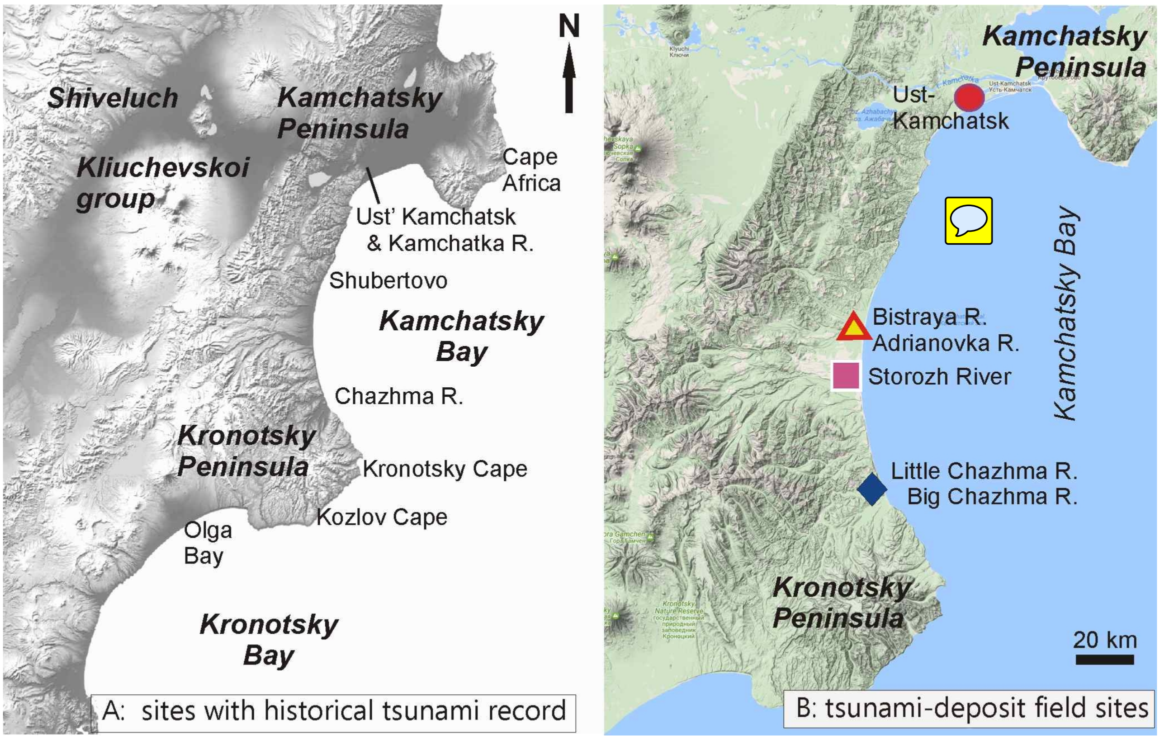

Figure S2. Left: sites in the field region with historical tsunami records, shown in Table S1. **Right:** field sites in south Kamchatsky Bay as well as location of Ust Kamchatsk field site (Pinegina et al. 2012; Pinegina, 2014) with data displayed in following figures.

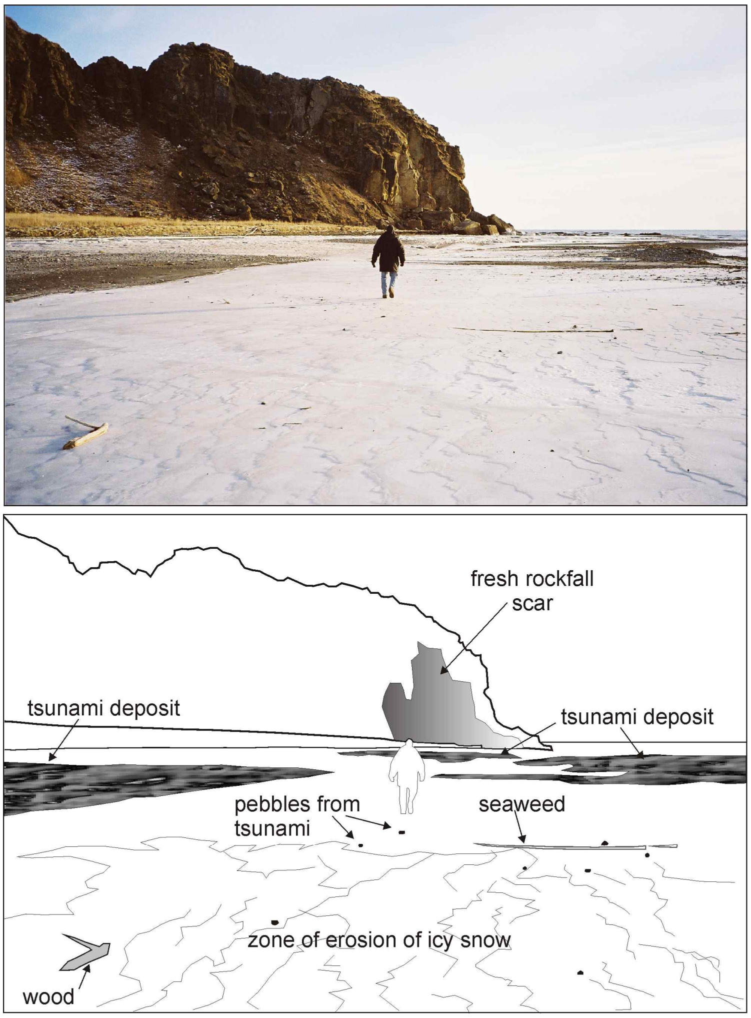

Figure S3. View of Kronotsky Cape during 9 December 1997 post-earthquake and post-tsunami survey, with sketch to label features; photo T. Pinegina. Modified from Pinegina et al. (2003).

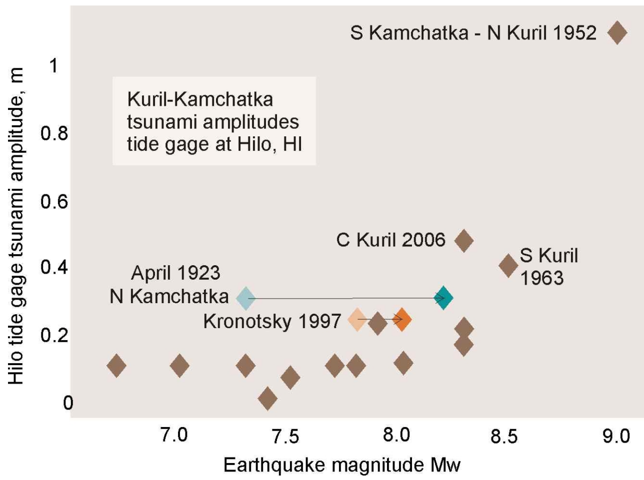

Figure S4. Tsunamigenic earthquakes from Kuril-Kamchatka subduction zone and their Hilo tide gage amplitude. Plotted from data in Table S3. April 1923 earthquake is reinterpreted by Gusev and Shumilina (2004) to be a magnitude 8.2 (see Fig. S2), plotted as darker blue. Kronotsky 1997 is plotted in light tan at 7.8 and dark tan as 8.0, which fits the tide-gage trend better, but not so convincingly as the 1923 April revision. “C Kuril” – Central Kuril.

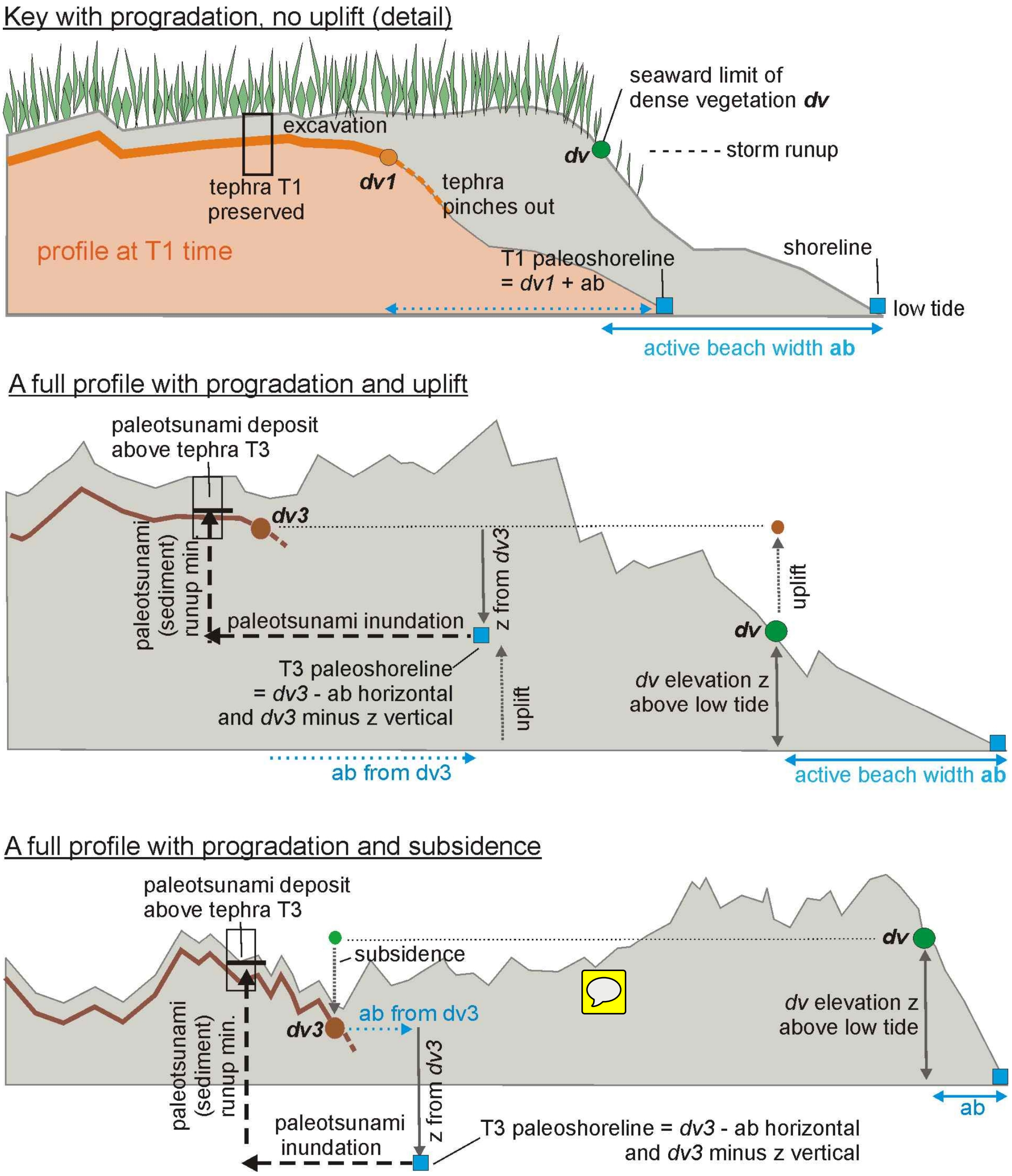

Figure S5. Idealized cartoons showing means for reconstructing paleoshorelines on profiles, using preserved tephra (as in Pinegina et al., 2013; MacInnes et al., 2016). The upper diagram is schematic of about 100 m width of shoreline (revised from Pinegina et al., 2013). The middle profile is based on Chazhma 220, about 350 m wide, maximum height about 8 m. The lower profile is from the Storozh 002, about 600 m wide, maximum height about 6 m. While these drawings are based on actual profiles, the illustrations are schematic and the tephra are not actual examples. Shorelines and their paleo-equivalents are shown as blue boxes in these 2-D views. The other primary reference point ***dv*** is the elevation above low tide of the first dense vegetation. The upper detail shows that it is near ***dv*** that tephra are preserved shoreward and not preserved seaward. From ***dv*** on any profile, we can measure down to low tide (vertical distance z) and seaward to the shoreline (horizontal distance ab). To reconstruct a paleoshoreline, we find a paleo ***dv*** and apply the modern metrics of elevation and distance from the shoreline to place a paleoshoreline point, from which we can use a tsunami deposits to estimate paleotsunami (sediment) inundation and runup. These shoreline reconstructions are made for each tephra interval, that is, we locate where a tephra such as tephra 3 pinches out, and all tsunami deposits above that tephra but below the overlying one are treated with the same approximation of paleoshoreline location.

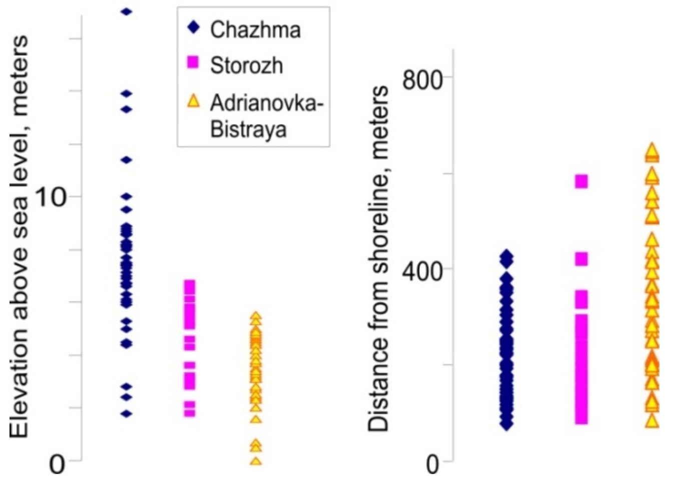

Figure S6. Distribution of elevations (meters above sea level) and distances (meters from modern shoreline) of excavations in the field area, southern Kamchatsky Bay, as originally compiled by Pinegina (2014). We use these distances and elevations for reconstructing tsunami sediment runup and inundation for 20th century tsunami deposits (Fig. S7). Note that the Chazhma area has higher elevations and narrower beach plains, and that the average elevations decrease northward (Chazhma to Bistraya), while the average beach plain width increases. In all, for example, there is only one excavation higher than 16 m, and only four excavations higher than 10 m. There are no excavations farther from the modern shoreline than about 600 m. Locations with symbols in Fig. S2.

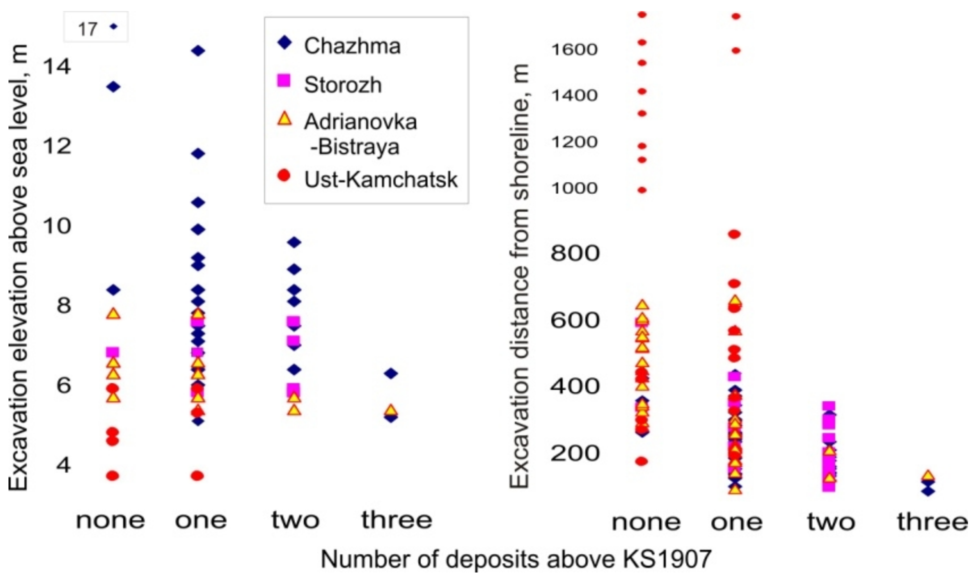

Figure S7. Elevation and distance of tsunami deposits above KS_{1907}, including data from the Ust' Kamchatsk area, north Kamchatsky Bay (Pinegina et al., 2012; Pinegina, 2014). In cases where there is only one deposit, it is the one not far stratigraphically above KS_{1907}, and thus which we interpret to have been deposited in 1923. This deposit reaches greater elevations and distances inland, being the largest 20th century tsunami in this bay. In cases where there are two deposits, the one in addition was at the surface in A.D. 2000 summer and is interpreted to be from the December 1997 Kronotsky tsunami. In a few excavations, there is a third, thin deposit between the other two, which we interpret to have been deposited by Chile 1960 tsunami (see Table S1). Locations with symbols in Figure S2.

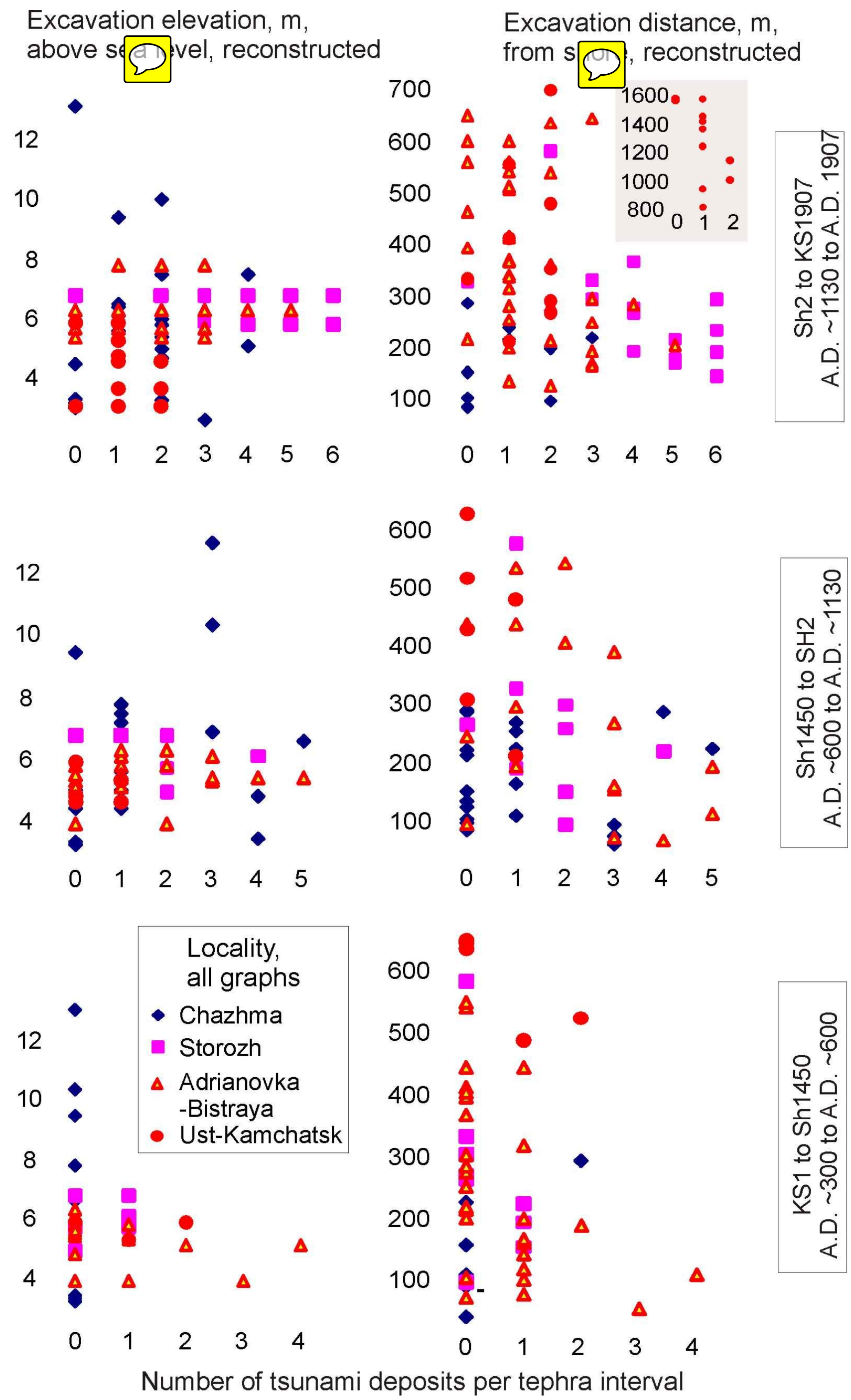

Figure S8. Number of paleotsunami deposits per tephra interval for three intervals below KS_{1907} (for 20^{th} century, see Fig, S7), including data from north Kamchatsky Bay near Ust-Kamchatsk (Pinegina et al., 2012; Pinegina, 2014). For each interval, the elevation and distance from shoreline of each excavation is reconstructed using methods as in Fig, S5. Locations with symbols in Fig. S2.

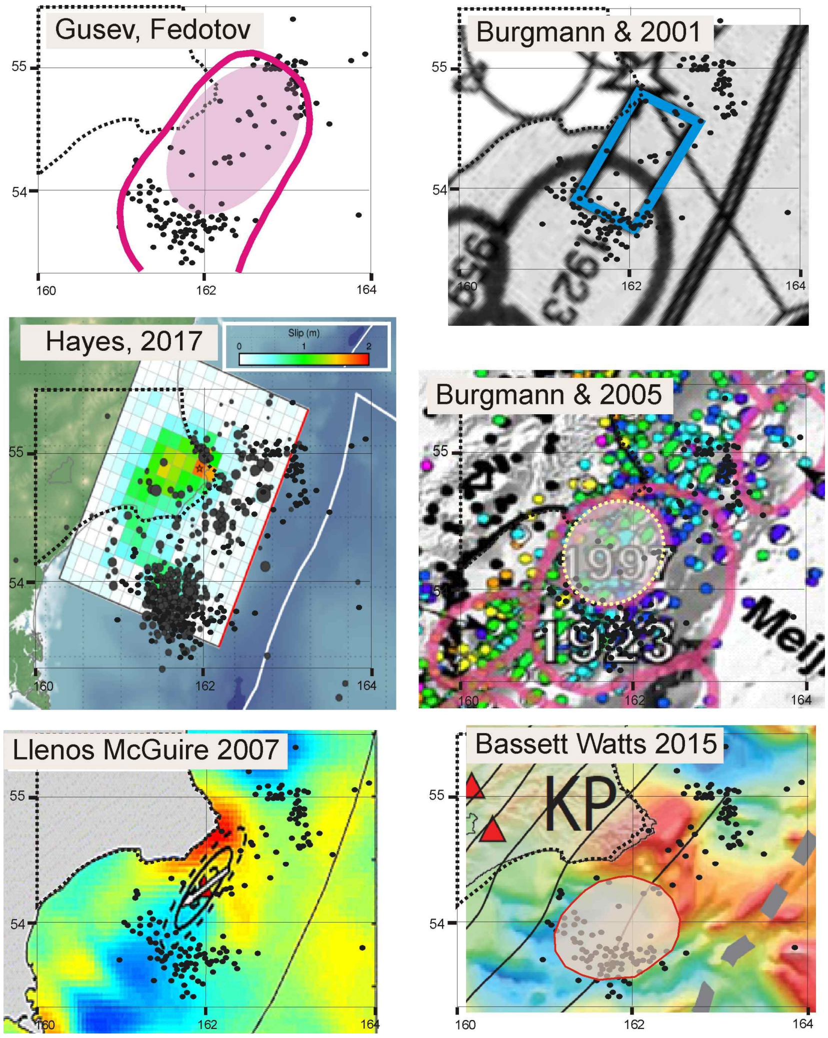

Figure S9. Rough comparison of rupture locations of the 5 December 1997 earthquake, all using the same base map with plotted aftershocks (traced from Gusev et al., 1998). Maps are scaled to the latitude and longitude of that base map (upper left) or fitted to the peninsula outline; because different map projections are used, this comparison is rough; maps are lined up vertically and horizontally. Not all symbols and scales are shown, only ones important to earthquake location and nature.

From upper left, counter-clockwise: **Gusev, Fedotov**: Gusev (2004) (Fig. S1) chose to outline the entire aftershock area as a rupture zone for the earthquake (dark pink outline), whereas Fedotov et al. (1998) did not draw an outline but interpreted that the earthquake filled a gap between the February and April 1923 events, which is approximated by the transparent pink ellipse. **Bürgmann et al. 2001**: Based on their dislocation model *Bcos* based on GPS measurements; rectangle is surface projection of the model fault. **Bürgmann et al. 2005**: [background is instrumentally recorded seismicity]; original figure caption states: "Bold red outlines labeled with year are the rupture zones of large historic earthquakes determined from aftershock distributions [Johnson and Satake, 1999]"; however, that 1999 reference does not mention or plot the 1997 Kronotsky earthquake, and the rupture zones are from Fedotov et al. 1982, from which Johnson and Satake omit the April 1923 event and misplot 1917 (to the north of this map zone). **Bassett and Watts 2015:** Ellipse (superimposed trace) is identified as "Coseismic slip/aftershock zone…" of the 1997 Kronotsky earthquake "modified from Bürgmann et al [2005]" Background is residual bathymetry, the positive features associated with the Emperor Seamount chain impinging on Kronotsky Peninsula (KP). **Llenos and McGuire 2007**: Characteristic rupture ellipses for the 1997 Kronotsky earthquake with major axes of length 0.5 Lc (inner dashed ellipse), 1 Lc (solid black ellipse) and 1.5 Lc (outer dashed ellipse) (Lc is characteristic rupture length) plotted on a TPGA (trench-parallel gravity anomaly) map; rupture directivity (arrow), centroid location (triangle); thin black line is trench axis. **Hayes 2017** (also see https://earthquake.usgs.gov/earthquakes/eventpage/usp0008btk#finite-fault): from finite fault modeling: Surface projection of modeled 1997 slip distribution superimposed on GEBCO bathymetry; modeling used a hypocenter matching or adjusted slightly from the initial NEIC solution (Lon. = 162.0 deg.; Lat. = 54.8 deg., Dep. = 34.0 km), and a fault plane defined using either the rapid W-Phase moment tensor (for near-real time solutions), or the gCMT moment tensor (for historic solutions). White line: plate boundary, gray circles are aftershock locations (up to 7 days), sized by magnitude.

References for supplementary material

Bassett, D. and Watts, A. B.: Gravity anomalies, crustal structure, and seismicity at subduction zones: 1. Seafloor roughness and subducting relief, Geochemistry, Geophysics, Geosystems, 16, 1508-1540, doi/10.1002/2014GC005684, 2015.

Bürgmann, R., Kogan, M.G., Levin, V.E., Scholz, C.H., King, R.W. and Steblov, G.M.: Rapid aseismic moment release following the 5 December, 1997 Kronotsky, Kamchatka, earthquake, Geophys. Res. Lett., 28, 1331-1334, doi: 10.1029/2000GL012350, 2001.

Bürgmann, R., Kogan, M.G., Steblov, G.M., Hilley, G., Levin, V.E. and Apel, E.: Interseismic coupling and asperity distribution along the Kamchatka subduction zone, J. Geophys. Res., 110, B07405, doi/10.1029/2005JB003648, 2005.

Engdahl, E. R., Villasenor, A.: Global seismicity: 1900-1999: in W.H.K. Lee, H. Kanamori, P.C. Jennings and C. Kisslinger, eds., International Handbook of Earthquake and Engineering Seismology, Part A, Ch. 41, 2002, 665-690. Academic Press. Accessed online Feb 2010. http://earthquake.usugs.gov/research/data/centennial.php

Fedotov, S.A., Chernyshev, S.D., Matviyenko, Y.D., and Zharinov, N.A.: Prediction of Kronotskoye earthquake of December 5, 1997, M = 7.8-7.9, Kamchatka, and its strong aftershocks with M > or = 6, Volcanology and Seismology, 6, 3-16, 1998, [in Russian].

Gusev, A. A.: The schematic map of the source zones of large Kamchatka earthquakes of the instrumental epoch: in Complex seismological and geophysical researches of Kamchatka. To 25th Anniversary of Kamchatkan Experimental & Methodical Seismological Department^ Ed. by E.I. Gordeev,V.N. Chebrov. Petropavlovsk-Kamchatsky, 445 pp., 2004 [in Russian].

Gusev, A. A., Levina, V. I., Saltykov, V. A., Gordeev, E .I.: Large Kronotskoye earthquake of Dec. 5, 1997: basic data, seismicity of the epicentral zone, source mechanism, macroseismic effects: in Gordeev et al., eds., 32-54, 1998 [In Russian with English abstract and figure captions].

Gusev, A. A., Shumilina, L. S.: Recurrence of Kamchatka strong earthquakes on a scale of moment magnitudes: Izvestiya, Physics of the Solid Earth, 40, 206-215, 2004.

Hayes, Gavin P.: The finite, kinematic rupture properties of great-sized earthquakes since 1990, Earth and Planetary Science Letters, 468, 94-100, doi: https://doi.org/10.1016/j.epsl.2017.04.003, 2017.

Llenos, A. L., and McGuire, J. J.: Influence of fore- arc structure on the extent of great subduction zone earthquakes, Journal of Geophysical Research: Solid Earth, 112, B09301, doi:10.1029/2007JB004944, 2007.

Luneva, M. N., Lee, J. M.: Shear wave splitting beneath South Kamchatka during the 3-year period associated with the 1997 Kronotsky earthquake, Tectonophysics, 374, 135-161, doi:10.1134/S1819714016040059, 2003.

NCEI, National Centers for Environmental Information (formerly NGDC), Natural Hazards Data, Images and Education, Tsunami and Earthquake databases: https://www.ngdc.noaa.gov/hazard/hazards.shtml

MacInnes, B., Kravchunovskaya, E., Pinegina, T., Bourgeois, J.: Paleotsunamis from the central Kuril Islands segment of the Japan-Kuril-Kamchatka subduction zone, Quaternary Research, 86, 54–66, https://doi.org/10.1016/j.yqres.2016.03.005, 2016.

Pinegina T. K.: Time-space distribution of tsunamigenic earthquakes along the Pacific and Bering coasts of Kamchatka: insight from paleotsunami deposits, Doctor of Geological Science dissertation, Institute of Oceanology RAS, Moscow, 235 pp., 2014 [in Russian].

Pinegina, T. K., Bazanova, L. I.: New data on characteristics of historical tsunamis on the coast of Avacha Bay (Kamchatka), Bulletin of Kamchatka regional association "Educational-scientific center". Earth sciences, 3, 5-17, 2016 [in Russian with English abstract].

Pinegina, T.K., Bourgeois, J., Bazanova, L.I., Melekestsev, I.V., and Braitseva, O.A.: A millennial-scale record of Holocene tsunamis on the Kronotsky Bay coast, Kamchatka, Russia, Quaternary Res., 59, 36-47, DOI: https://doi.org/10.1016/S0033-5894(02)00009-1, 2003

Pinegina, T.,K., Bourgeois, J., Kravchunovskaya, E. A., Lander, A.V., Arcos, M. E., Pedoja, K. and MacInnes B.T.: A nexus of plate interaction: Vertical deformation of Holocene wave-built terraces on the Kamchatsky Peninsula (Kamchatka, Russia), Geological Society of America Bulletin , 125, 1554-1568, doi: 10.1130/B30793.1, 2013.

Pinegina, T. K., Kozhurin, A. I., Ponomareva, V. V.: Seismic and tsunami hazard assessment for Ust-Kamchatsk settlement, Kamchatka, based on paleoseismological data, Bulletin of Kamchatka regional association "Educational-scientific center". Earth sciences. 1, 138-159, 2012 [in Russian with English abstract].

Pinegina, T. K., Kozhurin, A. I., Ponomareva, V. V.: Active Tectonics and Geomorphology of the Kamchatsky Bay Coast in Kamchatka, Russian Journal of Pacific Geology, 8, 65–76, 10.1134/S1819714014010047, 2014.

Slavina, L. B., Pivovarova, N. B., Levina, V. I.: A study in the velocity structure of December 5, 1997, Mw = 7.8 Kronotskii rupture zone, Kamchatka, J. Volcanology & Seismology, 1, 254-262, doi:10.1134/S0742046307040045, 2007.

Sohn, S.W.: The 1997 Kamchatka earthquake. Individual Studies by Participants at the International Institute of Seismology and Earthquake Engineering, 34, 91-99, 1998. PB: International Institute of Seismology and Earthquake Engineering.

Zayakin, Yu. A., Luchinina, A.A.: Catalogue tsunamis on Kamchatka, Obninsk: VNIIGMI-MTSD, 51pp., 1987 [Booklet in Russian].

Zobin, V. M., Levina, V. I.: The rupture process of the Mw 7.8 Cape Kronotsky, Kamchatka, earthquake of 5 December 1997 and its relationship to foreshocks and aftershocks, Bull. Seis. Soc. Am., 91, 1619-1628, doi: 10.1785/0119990116, 2001.